NMDA-Type Glutamate Receptor Activation Promotes Vascular Remodeling and Pulmonary Arterial Hypertension

Sébastien Dumas, Gilles Bru-Mercier, Audrey Courboulin, Marceau Quatredeniers, Catherine Rucker-Martin, Fabrice Antigny, Morad Nakhleh, Benoît Ranchoux, Elodie Gouadon, Maria-Candida Vinhas, et al.

Circulation

ORIGINAL RESEARCH ARTICLE

NMDA-Type Glutamate Receptor Activation Promotes Vascular Remodeling and Pulmonary Arterial Hypertension

Editorial, see p 2390

Sébastien J. Dumas, PharmD, PhD
Gilles Bru-Mercier, PhD
Audrey Courboulin, PhD
Marceau Quatredeniers, MSc
Catherine Rücker-Martin, PhD
Fabrice Antigny, PhD
Morad K. Nakhleh, PhD
Benoit Ranchoux, PhD
Elodie Gouadon, PhD
Maria-Candida Vinhas, BSc
Matthieu Vocelle, BSc
Nicolas Raymond, MSc
Peter Dorfmüller, MD, PhD
Elie Fadel, MD, PhD
Frédéric Perros, PhD
Marc Humbert, MD, PhD
Sylvia Cohen-Kaminsky, PhD

BACKGROUND: Excessive proliferation and apoptosis resistance in pulmonary vascular cells underlie vascular remodeling in pulmonary arterial hypertension (PAH). Specific treatments for PAH exist, mostly targeting endothelial dysfunction, but high pulmonary arterial pressure still causes heart failure and death. Pulmonary vascular remodeling may be driven by metabolic reprogramming of vascular cells to increase glutaminolysis and glutamate production. The *N*-methyl-D-aspartate receptor (NMDAR), a major neuronal glutamate receptor, is also expressed on vascular cells, but its role in PAH is unknown.

METHODS: We assessed the status of the glutamate-NMDAR axis in the pulmonary arteries of patients with PAH and controls through mass spectrometry imaging, Western blotting, and immunohistochemistry. We measured the glutamate release from cultured pulmonary vascular cells using enzymatic assays and analyzed NMDAR regulation/phosphorylation through Western blot experiments. The effect of NMDAR blockade on human pulmonary arterial smooth muscle cell proliferation was determined using a BrdU incorporation assay. We assessed the role of NMDARs in vascular remodeling associated to pulmonary hypertension, in both smooth muscle-specific NMDAR knockout mice exposed to chronic hypoxia and the monocrotaline rat model of pulmonary hypertension using NMDAR blockers.

RESULTS: We report glutamate accumulation, upregulation of the NMDAR, and NMDAR engagement reflected by increases in GluN1-subunit phosphorylation in the pulmonary arteries of human patients with PAH. K_v channel inhibition and type A-selective endothelin receptor activation amplified calcium-dependent glutamate release from human pulmonary arterial smooth muscle cell, and type A-selective endothelin receptor and platelet-derived growth factor receptor activation led to NMDAR engagement, highlighting crosstalk between the glutamate-NMDAR axis and major PAH-associated pathways. The platelet-derived growth factor-BB-induced proliferation of human pulmonary arterial smooth muscle cells involved NMDAR activation and phosphorylated GluN1 subunit localization to cell-cell contacts, consistent with glutamatergic communication between proliferating human pulmonary arterial smooth muscle cells via NMDARs. Smooth-muscle NMDAR deficiency in mice attenuated the vascular remodeling triggered by chronic hypoxia, highlighting the role of vascular NMDARs in pulmonary hypertension. Pharmacological NMDAR blockade in the monocrotaline rat model of pulmonary hypertension had beneficial effects on cardiac and vascular remodeling, decreasing endothelial dysfunction, cell proliferation, and apoptosis resistance while disrupting the glutamate-NMDAR pathway in pulmonary arteries.

CONCLUSIONS: These results reveal a dysregulation of the glutamate-NMDAR axis in the pulmonary arteries of patients with PAH and identify vascular NMDARs as targets for antiremodeling treatments in PAH.

Key Words: endothelin-1 ■ glutamate ■ NMDA receptor ■ platelet-derived growth factor ■ pulmonary arterial hypertension ■ smooth muscle cell ■ vascular remodeling

Sources of Funding, see page 2387

http://circ.ahajournals.org

Clinical Perspective

What Is New?

- Pulmonary vascular cell are equipped for glutamatergic communication. In pulmonary arterial hypertension (PAH), glutamate accumulates and the *N*-methyl-D-aspartate receptor (NMDAR, mainly known in the central nervous system, is overexpressed and overactivated in remodeled pulmonary arteries.
- Endothelin-1, upregulated in PAH, triggers both glutamate release and NMDAR mobilization at the cell membrane in smooth muscle cells.
- Platelet-derived growth factor, upregulated in PAH, triggers NMDAR mobilization at the cell membrane, and NMDAR antagonists inhibit platelet-derived growth factor-dependent smooth muscle cell proliferation.
- Smooth muscle cell NMDAR contributes to the development of experimental pulmonary hypertension, and pharmacological inhibition of NMDAR modulates hemodynamics, vascular and cardiac remodeling, and pulmonary hypertension.

What Are the Clinical Implications?

- In PAH, NMDAR signaling is dysregulated and is at the crossroads of known pathophysiological signaling pathway, such as the PDGF and endothelin-1 pathways, thus pointing to NMDAR as a potential therapeutic target.
- Pharmacological inhibition of NMDAR could be considered a therapeutic antiremodeling strategy in PAH. This would be made possible through the ongoing development of peripheral NMDAR antagonists (that do not cross the blood-brain barrier), thus avoiding central effects.

Pulmonary arterial hypertension (PAH) is a rare, devastating disorder characterized by chronic precapillary pulmonary hypertension, defined as high mean pulmonary arterial pressure (≥25 mm Hg at rest) with a normal pulmonary capillary wedge pressure (<15 mm Hg) and high pulmonary vascular resistance (>3 wood units), leading to breathlessness, loss of exercise capacity and, ultimately, right ventricular failure and death.[1] In PAH, the rise of pulmonary arterial pressure is associated with an intense vascular remodeling and inflammation of small pulmonary arteries, leading to their progressive obliteration.[2] PAH is currently treated with endothelin receptor antagonists, phosphodiesterase inhibitors, and prostacyclin analogs. These drugs improve quality of life and symptoms, decreasing pulmonary vascular resistance, mostly by acting on the vasoconstriction/vasodilation balance, but they cannot halt disease progression, reverse or cure this condition, even in new strategies based on drug combinations.[1,3] No clear antiremodeling strategy has been approved for PAH, and improvements in our understanding of the pathological mechanisms at work are required to drive the discovery of new targets for PAH treatment.[4]

Progressive pulmonary vessel obstruction may be driven by in situ thrombosis, endothelial dysfunction, sustained vasoconstriction, endothelial-to-mesenchymal transition, extracellular matrix synthesis, recruitment and differentiation of progenitor cells, cancer-like proliferation and apoptosis resistance of vascular cells, perivascular inflammation and autoimmunity, and dysregulation of vascular cell metabolism.[2,5] During the past few years, metabolic reprogramming has been suggested to underlie the hyperproliferative and apoptosis-resistant phenotype of pulmonary vascular cells associated with vascular remodeling in PAH.[6] This metabolic dysregulation results in a cancer-like glycolytic shift toward aerobic glycolysis, the so-called Warburg effect, and increases in fatty acid oxidation and glutaminolysis.[6–8] The increase in glutaminolysis involves increases in glutaminase (GLS1) expression and glutamine uptake by the PAH vasculature, resulting in greater glutamate production by pulmonary vascular cells, driving experimental pulmonary hypertension (PH).[8,9] Like cancer cells, pulmonary vascular cells in PAH use glutamate in an anaplerotic reaction to generate α-ketoglutarate for the tricarboxylic acid cycle.[8,9] Glutamate is actually a pleiotropic molecule acting at the crossroads of metabolism and signaling. It may, therefore, also be released into the intercellular space, where it may activate glutamate receptors, triggering multiple signaling pathways in a context of cell-cell communication.[10] Glutamatergic communication through *N*-methyl-D-aspartate receptors (NMDARs) is known to occur in the central nervous system (CNS), where glutamate is the main excitatory neurotransmitter and plays a major role in neuron fate. However, such signaling may also occur outside the CNS, including the vascular system in particular, as cerebral and aortic endothelial (ECs) and smooth muscle cells (SMCs) express NMDARs.[10–19]

The NMDAR is a ligand-gated, voltage-dependent channel of the ionotropic glutamate receptor family, located at cell-cell contact sites particularly for excitatory neuronal synaptic communication in the CNS (for review, see Paoletti et al[20]). It has also been suggested to play a pathological role in chronic peripheral disorders, such as type 2 diabetes mellitus[13] and cancer.[21,22] Some cancer cells hijack the NMDAR for aberrant proliferation.[21] In animal models of cancer, NMDAR-specific antagonists inhibit cancer cell proliferation, greatly increasing animal survival by preventing tumor growth.[22,23] The targeting of peripheral NMDARs with specific antagonists may be beneficial in these conditions.

NMDAR activation in cerebral or aortic ECs contributes to endothelial barrier disruption, inflammatory

cell infiltration, oxidative stress, and proliferation,[14–17] whereas in aortic SMCs, it triggers proliferation and extracellular matrix remodeling.[18,19] All these processes are relevant to pulmonary vascular remodeling in PAH.[24] However, the role of the glutamate-NMDAR axis in the remodeled pulmonary vascular bed has not yet been investigated. We hypothesized that the dysregulation of glutamatergic communication via NMDAR between pulmonary vascular cells might be involved in the remodeling observed in PAH and could be targeted pharmacologically.

METHODS

The data that support the findings of this study are available from the corresponding author on reasonable request.

Study Design

We used several approaches to assess the role of NMDARs in vascular remodeling in PAH: in situ observations of the dysregulation of glutamatergic communication in isolated human and rat PH pulmonary arteries (PAs), in vitro detection of glutamate release from primary cultures of human pulmonary vascular cells and analysis of the role of NMDAR activation in PASMC proliferation, in vivo targeted knockout (KO) of NMDAR in SMCs in the hypoxic mouse model of PH, and the use of NMDAR antagonists in the monocrotaline (MCT) rat model of PH.

Human lung specimens were obtained from patients with PAH during lung transplantation and from control subjects during lobectomy or pneumonectomy for localized lung cancers. In control lung specimens, the PAs studied were located far away from the tumor areas. PAH was diagnosed by cardiac catheterization at the National Reference Center for PAH, in a program approved by our institutional ethics committee, Comité de Protection des Personnes Ile-de-France VII, and written informed consent for participation in the study was obtained (protocol N8CO-08-003, ID RCB: 2008-A00485-50). The clinical data for the patients are summarized in Table I in the online-only Data Supplement. Lung histology was assessed by a pathologist, after transplantation, and confirmed the diagnosis of PH subgroups.

Sample size was determined on the basis of state-of-the-art experimental setups and practicality. Suspected outlier values in cell culture experiments were investigated with Grubbs' test and were excluded from statistical analysis if a positive result was obtained. All in vitro cell culture experiments were performed at least 3 times unless otherwise stated.

In animal studies, sample size was based on general knowledge and experience with animal models of PH. Animals were randomized to experimental groups on the basis of weight at treatment initiation and for data collection. The final end point (day 21) was selected in advance for the measurement of all parameters. All animals were used in strict accordance with European Union regulations (directive 2010/63/UE) for animal experiments and our institution's guidelines for animal care and handling. The procedures performed on rats and mice were approved by the local ethics committee, CEEA26 (Animal Experimentation Ethics Committee no. 26) and the French Ministry of Higher Education and Research. In vivo experiments were performed twice unless otherwise stated. Only the assessments of cardiac and pulmonary adventitial inflammation, cardiac fibrosis, and cardiomyocyte hypertrophy in the in vivo MK-801 experiment were performed blind.

Experimental Methods

A detailed description of experimental methods is provided in the Materials and Methods in the online-only Data Supplement. Antibodies and primers used in the experiments are listed in Tables II and III in the online-only Data Supplement, respectively.

Statistics

Statistical analysis was performed with Prism 6 (GraphPad) and Excel (Microsoft) software. The specific tests used to determine significance are reported for each instance in the figure legends. For a detailed description of statistical approaches, see the Materials and Methods in the online-only Data Supplement.

RESULTS

Human PAs Display Glutamate-NMDAR Axis Dysregulation in PAH

We first investigated the possible dysregulation of the glutamate-NMDAR axis in the PAs of human patients with PAH (PAH hPAs). We showed, by mass spectrometry imaging, that glutamate levels were significantly higher in PAH hPAs than in control arteries, this difference being particularly marked in medial lesions (characterized by SMC hyperplasia) and in intimal and occluded lesions, despite greater variability (Figure 1A and 1B, Figures I and II in the online-only Data Supplement). Levels of glutamate were significantly high in small arteries (diameter <250 μm) (Figure IIIA and IIIB in the online-only Data Supplement). Levels of glutamine, the precursor of glutamate in the GLS reaction, were also higher in PAH hPAs, particularly in arteries >150 μm of diameter (Figure 1A and 1C, Figures I, II, IIIA, and IIIC in the online-only Data Supplement). There was no difference on the glutamate-to-glutamine ratio, except in small arteries (<150 μm diameter) in which the ratio was slightly but significantly increased (Figure IIID and IIIE in the online-only Data Supplement). These results suggest that glutamate may accumulate both secondary to high glutamine levels and to a higher production from glutamine particularly in small arteries.

We focused on NMDARs, the glutamate receptors involved in cancer cell and vascular cell proliferation.[15,19,21,22] NMDAR activation requires recruit-

ment to the cell membrane, anchoring and clustering mediated by PDZ scaffolding proteins, such as PSD-95.[20] We found that control hPAs and cultured control human pulmonary microvascular endothelial cells (hPMVECs) and human pulmonary arterial smooth muscle cells (hPASMCs) expressed *GRIN1* gene (encoding the obligatory subunit of NMDARs, GluN1), all *GRIN2* genes (encoding the modulatory subunits of NMDARs, GluN2A, GluN2B, GluN2C, and GluN2D), and *Dlg4* (encoding PSD-95) (Table IV in the online-only Data Supplement). The GluN1, GluN2A, and PSD-95 proteins were detected, in situ, in both vascular cell types in PAH hPAs (Figure IV in the online-only Data Supplement). Thus, pulmonary vascular cells are equipped for functional responses to glutamate through NMDARs. Then we studied NMDAR regulation in the context of PAH. GluN1 is common to all NMDAR subtypes. Therefore, its regulation plays an essential role in controlling the total NMDAR pool available for activation. PAH hPAs produced significantly larger amounts of the short GluN1 protein containing the C2′ splicing domain than control arteries, whereas no change was observed in the expression of the long GluN1 protein containing the C2 splicing domain (Figure 1D). *GRIN1* gene expression was higher in PAH hPAs, cultured hPASMCs, and cultured hPMVECs compared with controls, although without reaching statistical significance (fold change: 1.7, 3.4, and 2.5, respectively) (Figure V in the online-only Data Supplement). Posttranscriptional modifications, including GluN1 phosphorylation, are crucial for regulating NMDAR trafficking and subcellular localization. Phosphorylation of the Ser-896 residue of GluN1 regulates NMDAR activation in neurons through its involvement in NMDAR trafficking to the cell membrane and accumulation at synaptic sites.[25–27] Western blots showed Ser-896-phosphorylated GluN1 protein levels to be significantly higher in PAH hPAs than in control arteries for both GluN1 isoforms (C2 and C2′) (Figure 1E). The ratio of phosphorylated to total GluN1 indicated that increases in both the production and phosphorylation of GluN1 contributed to the higher levels of phosphorylated GluN1 depending on GluN1 splicing isoform (Figure 1F). These findings were confirmed in situ, with stronger GluN1 staining in both medial SMCs and ECs in PAH hPAs than in controls (Figure 1G). Moreover, Ser-896 phosphorylated GluN1 staining was stronger in lesion with SMC hyperplasia than in control or nonremodeled PAH arteries, suggesting that NMDAR engagement in PAH SMCs may contribute to medial hypertrophy (Figure 1G).

We conclude that glutamate accumulates in PAH hPAs, and that NMDAR GluN1 subunits are upregulated and hyperphosphorylated, especially in SMC-related remodeling lesions. The glutamate-NMDAR axis is, therefore, dysregulated in PAH hPAs.

K_v Channels and the Endothelin-1 Pathway Regulate Calcium-Dependent Glutamate Release From PASMCs

Cell-to-cell glutamatergic signaling requires a minimal set of specific presynaptic proteins to deliver glutamate efficiently to the intercellular space (Figure 2A). These presynaptic proteins include glutaminase (GLS1 and GLS2 encoded by *GLS1* and *GLS2*), the enzyme catalyzing glutamate (Glu) production from glutamine (Gln), and vesicular glutamate transporters (VGLUT1, VGLUT2, and VGLUT3 encoded by *SLC17A7*, *SLC17A6*, and *SLC17A8*), hallmarks of the glutamatergic phenotype in neurons,[28] which mediate the accumulation of glutamate in small secretory vesicles. We found that *GLS1* as previously described,[8] *GLS2*, and *SLC17A7* genes were expressed in both control hPAs and cultured control hPMVECs and hPASMCs (Table V in the online-only Data Supplement). The GLS1 and VGLUT1 proteins were observed in situ, in both hPMVECs and hPASMCs, in PAH hPAs (Figure VI in the online-only Data Supplement), consistent with the production and vesicular storage of a readily releasable pool of glutamate by pulmonary vascular cells. In presynaptic neurons, VGLUT+ vesicles release glutamate into the synaptic cleft, secondary to calcium signals. Using a real-time approach, we showed that the calcium ionophore ionomycin (30 μmol/L) triggered both calcium entry and glutamate release in hPMVECs and hPASMCs in the presence of external Ca^{2+} (Figure 2B and 2C), consistent with rapid calcium-dependent glutamate release. Therefore, both vascular cell types can produce and release glutamate, and they express the NMDAR together with its scaffolding protein, PSD-95, suggesting possible glutamatergic communication within hPAs.

The glutamate-NMDAR axis appeared to be dysregulated principally in SMC-related PAH lesions. Therefore, we investigated glutamate release from hPASMCs. Exposure to a glutamate transporter inhibitor (DL-TBOA, 100 μmol/L) for 2 hours led to an increase in glutamate levels in the hPASMC supernatant (Figure 2D), implying (1) that there are functional glutamate transporters for extracellular glutamate recapture, and (2) the spontaneous release of glutamate. In PAH, the combination of an overactivation of calcium influx-triggering pathways and lower resting membrane potential lead to higher calcium concentrations in hPASMCs,[29] potentially increasing their calcium-dependent glutamate release. Endothelin-1 (ET-1), an overexpressed EC-derived peptide with vasoconstrictor and mitogenic properties that contributes to PAH, triggers calcium influx in hPASMCs (Figure VII in the online-only Data Supplement), and glutamate efflux from nonneuronal cells.[30,31] Glutamate release from hPASMCs was significantly amplified in the presence of ET-1, particularly with TBOA (Figure 2E), and the ET-1 effect was dose-dependent (significant

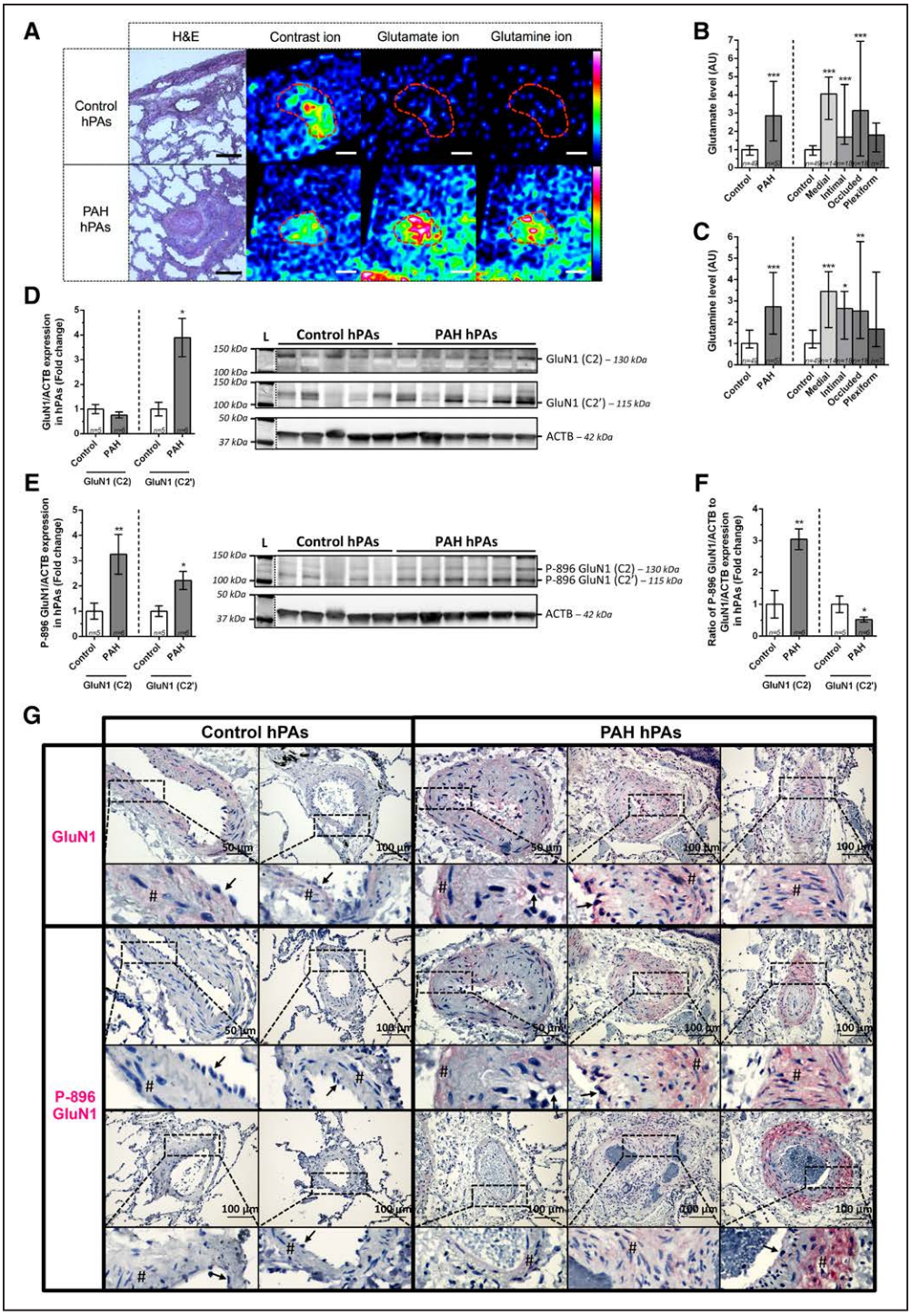

Figure 1. Both glutamate level and NMDAR expression/phosphorylation are increased in the pulmonary arteries of human patients with PAH.

A, Mass spectrometry imaging (MSI) of glutamate and glutamine in PAs from human controls (n=6) and patients with PAH (n=5). MSI imaging of a contrast ion (found at high concentration in arteries), glutamate, and glutamine ions in an artery from a control patient (**upper**) and in a remodeled artery from a patient with PAH (**lower**). Scale bar: 200 µm. Note that MSI acquisition and H&E staining were performed on adjacent sections. Thus, the contrast ion localization might not always completely match with the artery depicted on the H&E section. **B** and **C,** Quantification of glutamate (**B**) and glutamine (**C**) concentrations in human PAs from patients with PAH and controls. Quantification shown for all arteries (left: n=49 control hPAs, n=57 PAH hPAs) and subtypes of PAH arterial lesions (right: n=14 medial lesions, 18 neointimal lesions, 18 occluded lesions, and 7 plexiform lesions). **D, Right,** Western blot of GluN1 protein (C2 and C2′ isoforms) on lysates of isolated hPAs from patients with PAH and controls, with normalization relative to β-actin (ACTB). L indicates protein ladder. **D, Left,** Western blot quantification. (*Continued*)

from 100 pmol/L ET-1; Figure 2F). The addition of a type A-selective endothelin receptor (ET_AR) antagonist, BQ-123 (1 μmol/L), inhibited the effects of ET-1 on glutamate release, whereas a type B-selective endothelin receptor (ET_BR) antagonist, BQ-788 (1 μmol/L), did not (Figure 2G). ET-1-evoked glutamate release in hPASMCs is, therefore, mediated by ET_AR. In PAH hPASMCs, voltage-gated potassium (K_v) channel downregulation leads to a lower resting membrane potential followed by an increase in the activation of voltage-gated calcium channels and calcium influx, ultimately promoting a hyperproliferative and apoptosis-resistant phenotype and vasoconstriction.[32] We found that the K_v channel inhibitor 4-aminopyridine (4-AP, 3 mM) increased glutamate levels in the supernatant of hPASMCs and that this effect and the ET-1 effect were additive (Figure 2H).

Thus, both hPASMCs and hPMVECs can release glutamate in a rapid, calcium-dependent manner. In hPASMCs, K_v channels and the ET-1-ET_AR calcium influx-triggering pathway modulate this release, which suggests the possibility of more glutamate being released from hPASMCs in PAH.

NMDARs Are Engaged After ET_A or PDGF Receptor Activation and Contribute to Human PASMC Proliferation

The NMDAR is engaged in remodeled PAH hPAs, particularly in SMCs (Figure 1E and 1G). We therefore investigated the role of PAH-related pathways in NMDAR mobilization. In cultured control hPASMCs, ET-1 triggered Ser-896 GluN1 phosphorylation through ET_AR activation (Figure 3A). Thus, ET-1 amplifies glutamate release as well as engages the NMDAR. However, levels of Ser-896-phosphorylated GluN1 subunits were higher in hPAs from patients with PAH (Figure 1E), even those treated with endothelin receptor antagonists (see Table I in the online-only Data Supplement), suggesting the possible involvement of other pathways in NMDAR engagement.

Crosstalk between the NMDAR and PDGFR pathways occurs in neurons, with PDGF stimulation modulating NMDAR activity and directing the NMDAR response toward the proliferation-related MAPK (mitogen-activated protein kinase) and CREB (C-AMP Response Element-binding protein) pathways.[33] PDGF is a PASMC growth factor overproduced in PAH and involved in vascular remodeling.[34] We therefore investigated the potential of PDGF-BB to engage the NMDAR in hPASMCs. Exposure to PDGF-BB for 10 minutes triggered the phosphorylation of GluN1 Ser-896, demonstrating crosstalk between NMDAR and PDGFR in hPASMCs (Figure 3B). Phosphorylated GluN1 proteins were restricted to areas of cell-cell contact between hPASMCs, consistent with cell-cell glutamatergic communication via NMDARs in PDGF-BB-treated hPASMCs (Figure 3C). NMDAR activation promotes cell proliferation through the MAPK and Phosphoinositide 3-kinase (PI3K) pathways in aortic SMCs[19] and contributes to cancer cell proliferation.[21–23] We therefore investigated the role of NMDAR activation in hPASMC proliferation. We found that the noncompetitive NMDAR antagonists MK-801 and memantine inhibited the hPASMC proliferation induced by PDGF-BB (Figure 3D) or fetal bovine serum (Figure VIII in the online-only Data Supplement) in a dose-dependent manner.

Thus, in PAH, ET-1 and PDGF-BB may recruit NMDAR via GluN1 phosphorylation, and NMDAR activation is involved in hPASMC proliferation.

Smooth Muscle NMDAR Deficiency in Mice Attenuates Hypoxic Vascular Remodeling and Associated PH

We then investigated the potential role of PASMC NMDARs in vascular remodeling in the chronic hypoxia model of PH. We generated KO mice for NMDAR through the targeted deletion of *Grin1* in SMCs by a Cre/Lox approach. *Grin1* expression was weaker in the PAs of KO mice than in those of wild-type (WT) mice, demonstrating the efficacy of genetic recombination (Figure 4A, Figure IX in the online-only Data Supplement for genotyping). Age-matched KO and WT male mice were exposed to normoxia or hypoxia for 3 weeks to induce experimental PH (Figure IXB in the online-only Data Sup-

Figure 1 Continued. Values are expressed as fold change of the mean value relative to controls. **E, Right,** Western blot of Ser-896-phosphorylated GluN1 protein (C2 and C2′ isoforms) on lysates of isolated hPAs from patients with PAH and controls, with normalization relative to ACTB. L indicates protein ladder. **E, Left,** Western blot quantification. Values are expressed as fold change of the mean value relative to controls. **F,** Ratio of Ser896-phosphorylated GluN1-to-ACTB signal intensities divided by the ratio of GluN1-to-ACTB signal intensities from Western blots performed on isolated hPAs from patients with PAH and controls. Values are expressed as fold change of the mean value relative to controls. **G,** Transmitted light microscopy images of the GluN1 and Ser896-phosphorylated GluN1 proteins (red) on control PAs from a donor and from a patient with PAH. Hashtags indicate SMCs; and arrows, ECs. Sections are counterstained with hematoxylin (blue). Scale bar: 50 to 100 μm. Three independent experiments were performed on 3 patients with PAH and 3 controls. Statistical significance was determined in Mann-Whitney and Kruskal-Wallis tests followed by Dunn's test for multiple comparisons (**B, C, E Left,** and **F Right**) or unpaired Student *t* tests (**D, E Right,** and **F Left**). $^{*}P<0.05$; $^{**}P<0.01$; $^{***}P<0.001$ versus control. The values shown are medians±interquartile range (**B** and **C**) or means±SEM (**D** through **F**). EC indicates endothelial cell; hPA, human pulmonary artery; NMDAR, *N*-methyl-D-aspartate receptor; PA, pulmonary artery; PAH, pulmonary arterial hypertension; and SMC, smooth muscle cell.

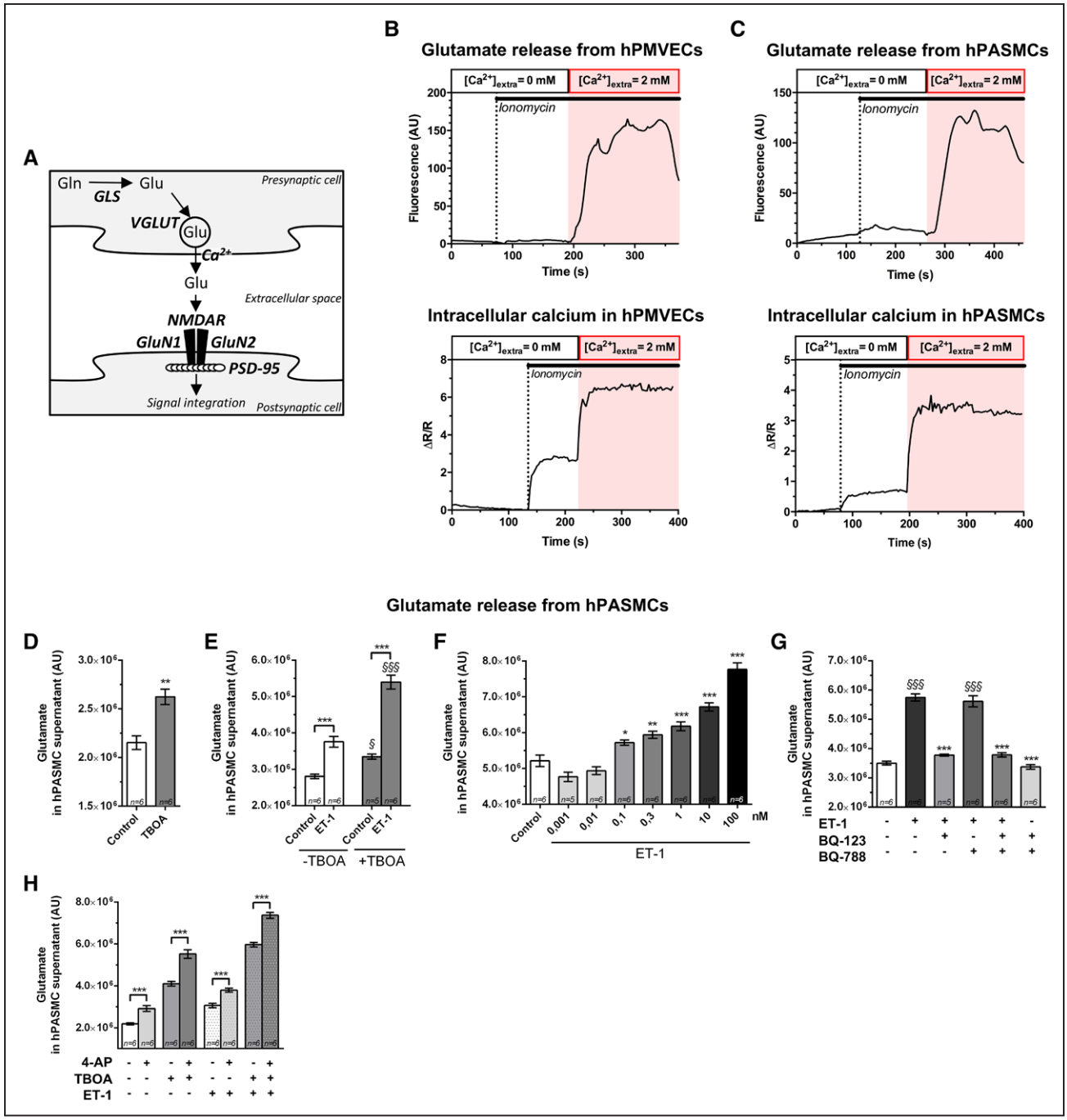

Figure 2. K_v channels and ET_A receptors modulate calcium-dependent glutamate release from human PASMCs. **A,** Summary of cell-cell glutamatergic communication mechanisms mediated by NMDARs. **B** and **C, Upper**, Real-time analysis of glutamate release from hPMVECs and hPASMCs based on a glutamate dehydrogenase (GDH)-linked assay. Typical traces of glutamate release from hPMVECs (**B**) and hPASMCs (**C**) after ionomycin exposure (30 μmol/L) in the presence or absence of extracellular Ca^{2+} (2 mM). **Lower,** Real-time measurement of intracellular calcium concentration (Fura-2 fluorescent probe) in cultured hPMVECs (**B**) and hPASMCs (**C**) from controls after ionomycin exposure (30 μmol/L) in the presence or absence of extracellular Ca^{2+} (2 mM). Values are expressed as ΔR/R, where R is the ratio between fluorescence signals for excitation at 340 nm and 380 nm, obtained before the addition of ionomycin, and ΔR is the difference between the ratios measured during a response to ionomycin and R. The intracellular calcium signal after ionomycin exposure in the absence of extracellular calcium is probably because of calcium release from internal stores. **D** through **H,** Measurement of extracellular glutamate released into the supernatant of cultured hPASMCs from controls with and without 2 hours of exposure to DL-TBOA, endothelin-1 (ET-1), or 4-aminopyridine (4-AP). **D,** Evaluation of the effect of DL-TBOA (a glutamate transporter inhibitor, 100 μmol/L) on glutamate release. **E,** Evaluation of the effect of ET-1 (100 nmol/L) on glutamate release in the presence or absence of DL-TBOA. **F,** Determination of the dose-response relationship for the effect of ET-1 (from 1 pmol/L to 100 nmol/L) (*Continued*)

plement). Normoxic KO and WT mice had similar right ventricular systolic pressures (RVSP) and left ventricular systolic pressures. By contrast, hypoxic KO mice had significantly lower RVSP values than hypoxic WT mice (Figure 4B), whereas left ventricular systolic pressures values did not differ between hypoxic WT and KO mice (Figure 4C). Echo-Doppler scans showed pulmonary artery acceleration time to be greater in hypoxic KO mice than in WT mice, whereas no difference was observed between normoxic KO mice and WT mice (Figure 4D). Normoxic KO and WT mice had similar right cardiac hypertrophy indices (Fulton index), whereas hypoxic KO mice displayed significantly lower Fulton index values than hypoxic WT mice (Figure 4E). Hypoxic KO mice had a lower right ventricle-to-body weight ratio than hypoxic WT mice, whereas left ventricle plus septum-to-body weight ratio did not differ between hypoxic KO and WT mice (Figure IXC and IXD in the online-only Data Supplement). Hypoxic KO mice also had poorer muscularization of the small pulmonary arterioles (external diameter <75 μm) than WT mice (Figure 4F). The muscularization of large arteries (external diameter from 75 μm to 125 μm) was also poorer in KO than in WT mice, regardless of oxygen conditions, suggesting a role for NMDARs in the physiological coverage of PAs with SMCs (Figure 4F). KO and WT mice displayed no significant differences in body weight and heart rate (Figure IXE and IXF in the online-only Data Supplement). Thus, NMDAR-KO in SMCs attenuates PH in hypoxic mice.

Together with our findings on the role of NMDARs in hPASMC proliferation, these results suggest that the NMDARs on PASMCs contribute to vascular remodeling in PH.

NMDAR Antagonists Have Beneficial Effects on PH in Vivo, Decreasing Vascular and Cardiac Remodeling in the MCT Rat Model

We then investigated the potential of NMDAR antagonists to prevent or reverse PH in the MCT rat model. The powerful NMDAR antagonist MK-801 was used in a curative protocol from day 14 (when rats typically present signs of right cardiac hypertrophy) to day 21 after MCT injection (Figures 5 and 6 and Figure X in the online-only Data Supplement). The clinically available low-affinity NMDAR antagonist memantine was used in a preventive protocol (from days 1 to 21 after MCT injection) (Figure XI in the online-only Data Supplement). MCT-treated rats receiving MK-801 presented central effects (ataxia, stereotypies, and hyperlocomotion, as previously reported[35]) and a lower body weight (Figure XA in the online-only Data Supplement) potentially accounted for by central effects,[36] but hemodynamic parameters, including mean pulmonary arterial pressure, RVSP, and total pulmonary resistance, had returned to almost normal values, contrasting with the findings for rats receiving vehicle alone (Figure 5A through 5C). Echo-Doppler scans from MK-801-treated MCT rats showed a greater pulmonary artery acceleration time than in untreated MCT rats, although not statistically significant (Figure 5D). By contrast with effects on RVSP, chronic administration of MK-801 had no significant effect on the systemic pressure (Figure XB in the online-only Data Supplement). Hemodynamic effects were associated with milder medial hypertrophy of the large PAs and a lower proportion of muscularized and occluded small arterioles (Figure 5E and 5F). Right ventricular hypertrophy was clearly reversed by MK-801 treatment, as demonstrated by the Fulton index and echocardiographic measurements of right ventricular thickness (Figure 5G and 5H). These findings were supported by the significant decrease in right ventricle-to-body weight ratio in MK-801 rats relative to MCT rats, whereas the left ventricle plus septum-to-body weight ratio was unaffected (Figure XC and XD in the online-only Data Supplement). Moreover, MK-801 significantly increased right ventricle fractional shortening, a surrogate for myocardial contractility (Figure 5I). These changes were associated with significant decreases in right ventricle cardiomyocyte diameter, cardiac fibrosis, and inflammatory cell infiltration (Figure 5J through 5L). By contrast, cardiac output was not significantly improved by MK-801 treatment (Figure XE in the online-only Data Supplement). However, cardiac output depends on both heart rate (unchanged by MK-801 treatment; see Figure XF in the online-only Data Supplement) and stroke volume, which is directly related to body surface area. The calculation of cardiac index (ie, cardiac output-to-body surface area ratio) may be useful for treatments affecting body weight, as for the MCT and MCT+MK-801 rat groups relative to controls. Cardiac index was significantly lower in MCT rats but

Figure 2 Continued. on glutamate release. **G,** Evaluation of the effects of an ET_A-R antagonist (BQ-123, 1 μmol/L) and an ET_B-R antagonist (BQ-788, 1 μmol/L) on ET-1 (10 nmol/L)-induced glutamate release. **H,** Evaluation of the effect of 4-AP (3 mM) on glutamate release in the presence or absence of DL-TBOA and ET-1.Statistical significance was determined in 1-way ANOVA with Bonferroni correction for multiple comparisons (**E** through **H**) or unpaired Student *t* tests (**D**). $^{*}P<0.05$; $^{**}P<0.01$; $^{***}P<0.001$ versus control (**D** and **F**) or versus ET-1 (**G**). $^{§}P<0.05$; $^{§§§}P<0.001$ versus TBOA (**E**) or control (**G**). The values shown are means±SEM. 4-AP indicates 4-aminopyridine; ET-1, Endothelin-1; ETA-R, Endothelin-type A receptor; ETB-R, Endothelin-type B receptor; Gln, glutamine; GLS, glutaminase; Glu, glutamate; hPASMC, human pulmonary arterial smooth muscle cell; hPMVEC, human pulmonary microvascular endothelial cell; NMDAR, *N*-methyl-D-aspartate receptor; PSD-95, Postsynaptic density protein 95, TBOA, threo-beta benzyloxyaspartate; and Vglut, Vesicular glutamate transporter.

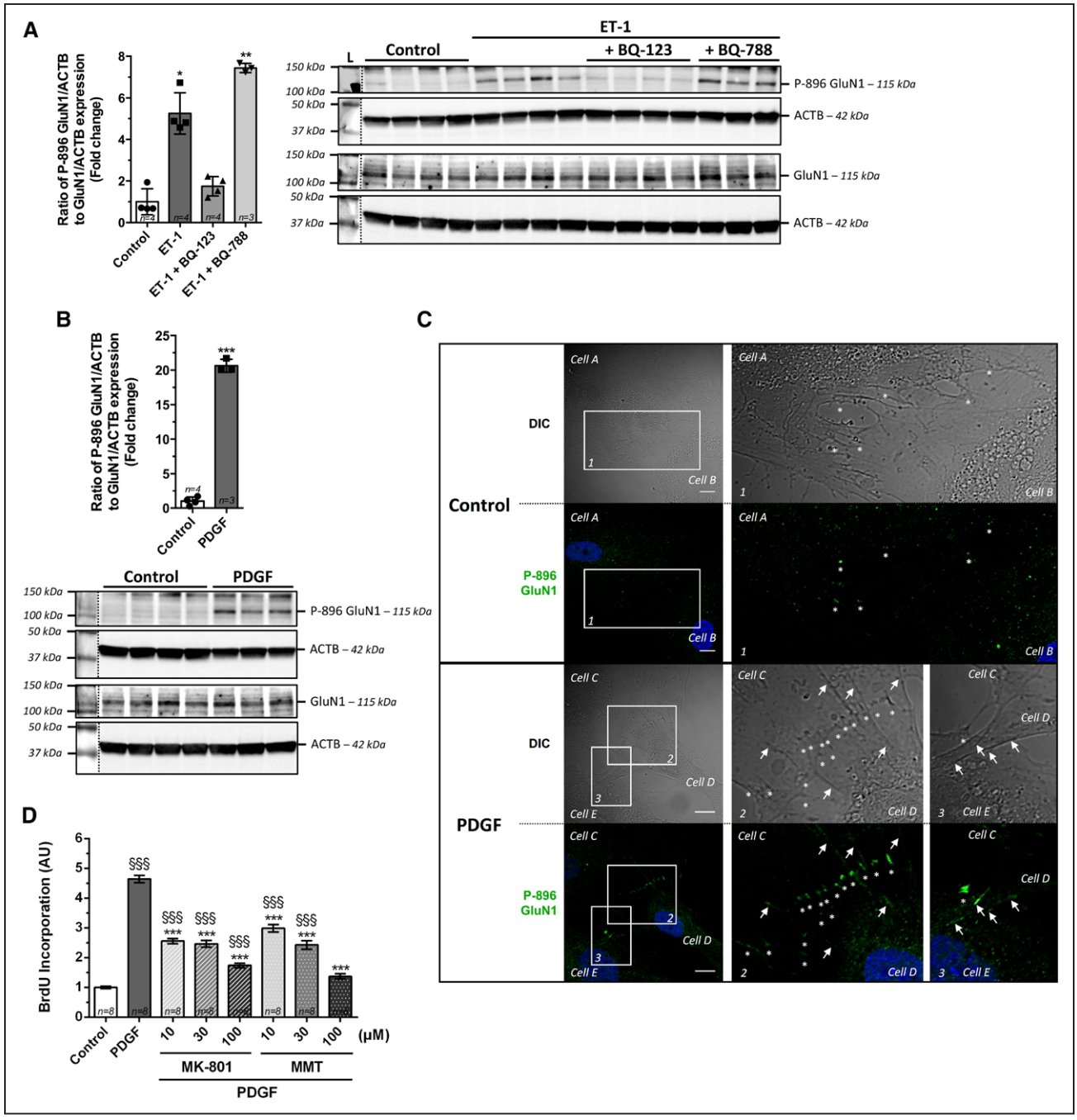

Figure 3. NMDAR engagement after ETAR or PDGFR activation: a role for NMDAR in hPASMC proliferation.
A and **B,** Western blot of Ser896-phosphorylated GluN1 and total GluN1 proteins on lysates from control hPASMC cultures. Cells were left unstimulated or were stimulated with (**A**) ET-1 (10 nmol/L) for 10 minutes in the presence or absence of 1 μmol/L BQ-123 or 1 μmol/L BQ-788 (**Left,** Western blot quantification), or (**B**) PDGF-BB (50 ng.ml^{-1}) for 10 minutes (**Upper,** Western blot quantification). L indicates protein ladder. Values are the ratio of signal intensities for Ser896-phosphorylated GluN1 and ACTB signal intensities divided by the ratio of signal intensities for GluN1 and ACTB, expressed as a fold change relative to the mean value for controls. **C,** Typical staining for Ser896-phosphorylated GluN1 protein (green) on cultured hPASMCs. Cells were left unstimulated or were stimulated with PDGF-BB (50 ng.ml^{-1}) for 10 minutes (**Upper,** untreated hPASMCs; **Lower,** PDGF-treated hPASMCs). For each set, both differential interference contrast (DIC) and Ser896-phosphorylated GluN1 staining images are shown. Higher magnifications are shown (numbered from 1–3). Asterisks indicate cluster-like staining at cell-cell contacts, whereas arrows indicate staining on filamentous projections from one cell to another. Scale bar: 10 μm. Three independent experiments were performed on 3 controls. **D,** Measurement of control hPASMC proliferation (BrdU incorporation) after exposure to PDGF-BB (10 ng.ml^{-1}) in the presence or absence of various concentrations of NMDAR antagonists (MK-801 or memantine [MMT], both at concentrations of 10 μmol/L to 100 μmol/L). (*Continued*)

not in MK-801-treated MCT rats when compared with control rats (Figure XG and XH in the online-only Data Supplement). Consistent with these results, a multiple linear regression analysis showed that the lower body weights of MK-801-treated MCT rats than of untreated MCT rats made no significant contribution to the results obtained for mean pulmonary arterial pressure, RVSP, total pulmonary resistance, and the Fulton index (Table VI in the online-only Data Supplement). The chronic administration of another NMDAR antagonist, memantine, yielding 24-hour plasma concentrations sufficiently high to block NMDAR (Figure XIA in the online-only Data Supplement), slowed PH development (Figure XIB through XIP in the online-only Data Supplement).

Thus, the administration of NMDAR antagonists can prevent or reverse PH in the MCT rat model, decreasing vascular remodeling, endothelial dysfunction, cardiac inflammation, and hypertrophy, and thereby having beneficial effects on hemodynamics.

The NMDAR Antagonist MK-801 Targets the Dysregulated Glutamate-NMDAR Pathway in the PAs of MCT Rats, Decreasing Proliferation, Apoptosis Resistance, Endothelial Dysfunction, and Perivascular Inflammation

We further explored the molecular mechanisms associated with the beneficial effects of the NMDAR antagonist MK-801 on vascular remodeling in the MCT rat model of PH. MK-801 irreversibly binds to the GluN1 subunit of the NMDAR. We therefore investigated its effects on GluN1 protein levels in isolated rat PAs (rPAs). Levels of both the C2 and C2′ GluN1 isoforms were higher in PAs from MCT rats than in those from controls, and MK-801 significantly normalized the levels of the C2′ GluN1 isoform, meanwhile reducing the levels of the C2 GluN1 isoform toward control values (Figure 6A). We also observed higher *Grin1* mRNA levels in PAs from MCT rats than in those from controls, although not statistically significant (P=0.07 versus control), and MK-801 treatment did not decrease *Grin1* gene expression (P=0.09 versus control, P>0.99 versus MCT) (Figure 6B). Thus, MK-801 treatment significantly decreased GluN1 protein levels without affecting *Grin1* mRNA levels in rPAs, suggesting that the GluN1 NMDAR subunit is degraded after irreversible binding to MK-801. We then studied the effect of MK-801 on GLS1 protein levels in rPAs. GLS1 protein levels were higher in PAs from MCT rats than in controls (Figure 6C),[8] and MK-801 treatment significantly decreased GLS1 levels in rPAs, suggesting that NMDAR activity regulates the production of its agonist (Figure 6C).

We further assessed, in rPAs, the effect of MK-801 treatment on the levels of proliferative cell nuclear antigen and survivin proteins as surrogates for proliferation and apoptosis resistance, respectively. Both markers were more strongly expressed in the PAs of MCT rats than in those of controls, and their levels were significantly decreased by MK-801 (Figure 6D and 6E), consistent with a vascular effect of NMDAR blockade on both proliferation and apoptosis-resistant phenotypes in PH. Moreover, serum soluble E-selectin concentration, a marker of endothelial dysfunction, was almost normalized by MK-801 treatment, whereas serum soluble ICAM-1 concentration was not significantly affected (Figure 6F, Figure XI in the online-only Data Supplement). Furthermore, MK-801 treatment completely eliminated macrophage infiltration from the PA adventitia without affecting the measured areas of adventitia (Figure 6G).

Thus, MK-801 treatment disrupted the overactivated glutamate-NMDAR pathway in PAs from MCT rats, and this effect was associated with decreases in proliferation, resistance to apoptosis, endothelial dysfunction, and perivascular inflammation.

DISCUSSION

We revealed dysregulation of the glutamate-NMDAR axis in PAH hPAs, involving known PAH-associated pathways and promoting pulmonary vascular remodeling. We found that glutamate and its precursor, glutamine, accumulated in PAH hPAs. During pulmonary hypertension, the vascular stiffness increases and triggers the overexpression of the glutamate-producing enzyme GLS1 in pulmonary vascular cells.[8] Moreover, the lung vasculature takes up large amounts of glutamine (the precursor of glutamate in the GLS reaction) in patients with PAH possibly because of *BMPR2* mutations.[9] Thus, vascular stiffness and *BMPR2* mutations may trigger the accumulation of glutamine and glutamate observed in PAH hPAs. Glutamate release is necessary for cell-cell glutamatergic communication in nonneuronal cells and has been implicated in diseases outside the CNS, such as diabetes mellitus[13] and some cancers.[21,23] We showed that

Figure 3 Continued. Values are normalized with respect to unstimulated cultures. Statistical significance was determined in Kruskal-Wallis tests followed by Dunn's test for multiple comparisons (**A**), unpaired Student *t* tests (**B**), or 1-way ANOVA with Bonferroni correction for multiple comparisons (**D**). $^{*}P$<0.05; $^{**}P$<0.01; $^{***}P$<0.001 versus control (**A** and **B**) or $^{§§§}P$<0.001 versus control; $^{***}P$<0.001 versus PDGF (**D**). The values shown are means±SD (**A** and **B**) or means±SEM (**D**). Plots of individual values are also shown (**A** and **B**). ACTB indicates beta-actin; ET-1, endothelin-1; ETAR, endothelin-type A receptor; hPASMC, human pulmonary arterial smooth muscle cell; NMDAR, N-methyl-D-aspartate receptor; PDGF, platelet-derived growth factor; and PDGFR, platelet-derived growth factor receptor.

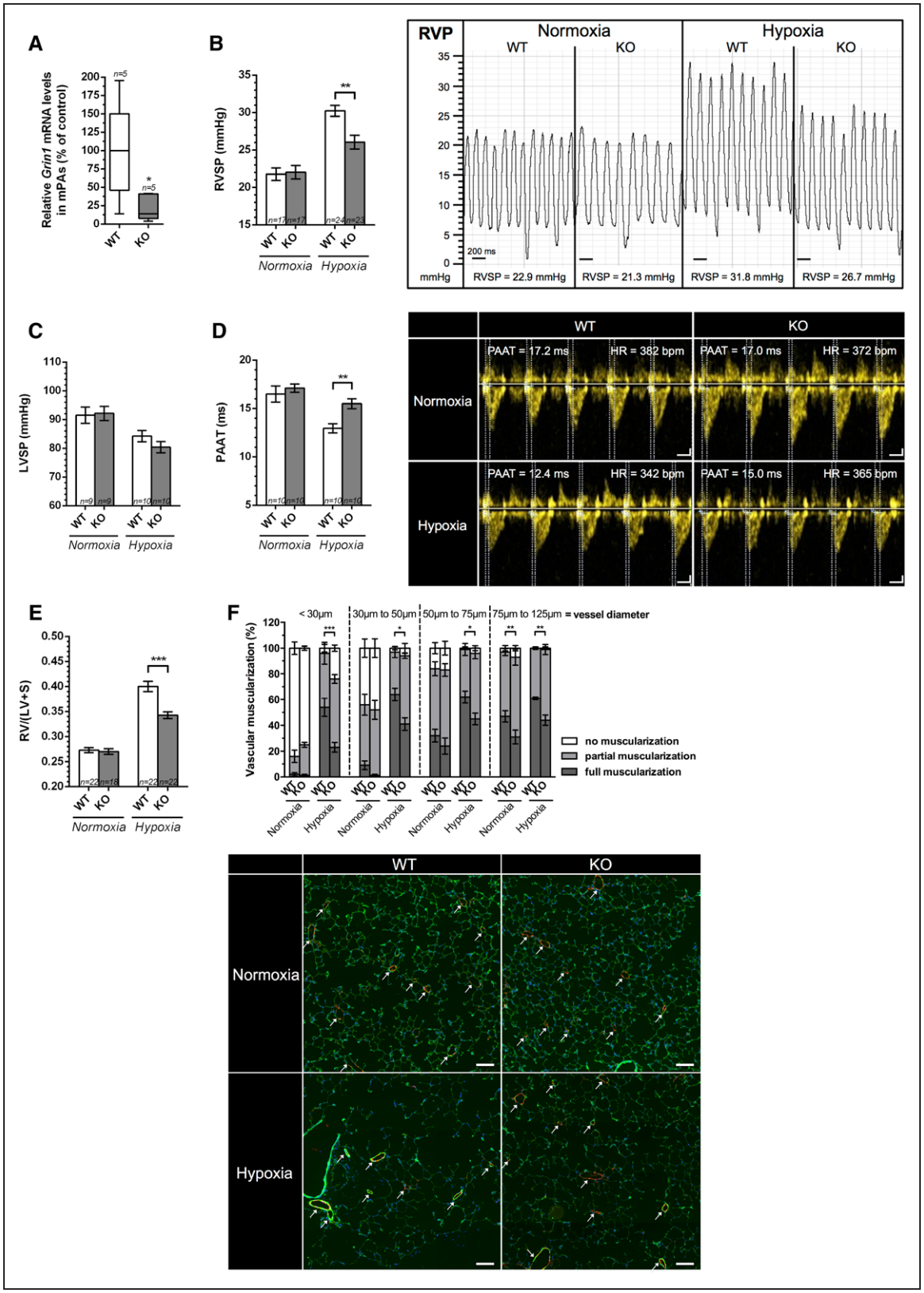

Figure 4. Role of smooth muscle cell NMDARs in vascular remodeling in the chronic hypoxia model of pulmonary hypertension.

A, Quantitative RT-PCR of *Grin1* on total RNA from isolated PAs from WT mice and mice with a KO of NMDAR in SMCs, with normalization relative to *Actb* gene expression. Values are normalized with respect to those of WT mice. **B,** Right ventricular systolic pressure (RVSP) measurement in WT and NMDAR-KO mice after 3 weeks of normoxia or chronic (*Continued*)

pulmonary vascular cells display rapid calcium-dependent glutamate release and that ET_AR activation or membrane depolarization through K_v channel inhibition enhances basal glutamate release from PASMCs. In PAH, pathways triggering calcium influx, such as ET-1 signaling[30] and K_v channel downregulation/*KCNK3* gene mutations (decreasing the resting membrane potential of PASMCs[37]), may increase glutamate release from PASMCs.

Little is known about glutamate signaling in the vascular system even though not only ECs and SMCs can release glutamate (our study), but also immune cells and platelets.[12,38,39] Moreover, vascular cells may express a wide range of glutamate receptors (NMDARs but also AMPA receptors and metabotropic glutamate receptors) that could mediate crucial roles for the function and development of the vascular system, such as regulating endothelial barrier permeability and angiogenesis.[39,40] Further studies are required to finely characterize the role of glutamate signaling through its different receptors in the context of cell-cell interaction inside the vascular wall or with other cells in the vicinity (immune cells, platelets, etc).

Although the synapse definition is mainly restricted to neuronal cells, synaptic-like communication has been suggested to occur also in nonneuronal cells, for instance, the immunologic synapse between an antigen-presenting cell and a lymphocyte/thymocyte, the epithelial synapse zonapse between epithelial cells, and the leukocyte/endothelial synapse.[12,41] Vascular cells express critical actors of synaptogenesis, especially adhesion molecules such as presynaptic neurexins and postsynaptic neuroligins that recruit glutamate vesicles and glutamate receptors, respectively, at cell membranes triggering synapse formation.[42] It is interesting to note that cerebellin-2, an alternative partner for neurexin, was shown overexpressed in lungs and ECs from patients with PAH.[43] Taken together with our results suggesting calcium-dependent vesicular glutamate release, the glutamatergic communication between vascular cells may occur in a synaptic-like manner. However, further studies are required to assess whether this cell-cell communication is synaptic- or extrasynaptic-like in vessels.

We found that pulmonary vascular cells expressed the NMDA-type glutamate receptor and that the GluN1 NMDAR subunit was upregulated in PAH hPAs and MCT rPAs. Inflammation mediated by the tumor necrosis factor α pathway and oxidative stress, both of which are features of PAH,[29] upregulates GluN1 expression in airway SMCs and brain ECs, respectively.[44,45] These mechanisms may also operate in pulmonary vascular cells in PAH. In PAH hPAs, NMDARs are also engaged through increases in the levels of Ser-896-phosphorylated GluN1. In the CNS, this phosphorylation is required for NMDAR exit from the endoplasmic reticulum and is also associated with higher levels of NMDARs in synapses, consistent with greater NMDAR trafficking to the cell membrane.[25–27] This finding is consistent with our results showing the localization of phosphorylated GluN1 subunits at cell-cell contacts in cultured hPASMCs. In these cells, phosphorylation was induced by PDGF-BB or ET-1 via ET_AR activation, endowing the NMDAR with a molecular hub function at the crossroads of known PAH-associated pathways.[29,30,34] NMDAR activation contributed to the PDGF- or fetal bovine serum-dependent proliferation of hPASMC and vascular remodeling. Furthermore, smooth muscle NMDAR-KO led to lower levels of hypoxic pulmonary vessel muscularization in mice, highlighting the role of PASMC NMDARs in vascular remodeling. In neurons, PDGFR/NMDAR crosstalk leads to proproliferative MAPK and CREB pathway activation.[33] Moreover, NMDAR activation induces the proproliferative MAPK and PI3K pathways in aortic SMCs.[19] The PASMC NMDAR overactivation observed in PAH may therefore contribute to PASMC overproliferation and vascular remodeling. NMDAR-KO, driven by the SM22α gene promoter, may also affect cardiomyocytes.[46] However, given the lack of effect of NMDAR-KO on most of the heart parameters measured (except right heart hypertrophy), NMDAR deficiency in mouse hearts is unlikely to have led to the exclusive attenuation of RVSP in hypoxia or even pulmonary vascular neomuscularization, which is a direct effect of hypoxia on the pulmonary vascular bed.[29]

Figure 4 Continued. hypoxia (FiO_2: 10%). **Right,** Representative traces of pressure variations in the right ventricle of wild-type and NMDAR KO mice in either normoxia or after hypoxia exposure. Scale bar: 200 ms. **C,** Left ventricular systolic pressure (LVSP) measurement in WT and NMDAR-KO mice after 3 weeks of normoxia or chronic hypoxia. **D,** Pulmonary artery acceleration time (PAAT) measured by echocardiography in pulsed-wave Doppler mode in WT and NMDAR-KO mice after 3 weeks of normoxia or chronic hypoxia. **Right,** Representative traces of blood velocity variations in the PA of WT and NMDAR-KO mice either in normoxia or after hypoxia exposure. Horizontal scale bar: 100 ms. Vertical scale bar: 10 cm/s. **E,** Ratio of right ventricle weight to left ventricle plus septum weight (Fulton index) for WT and NMDAR-KO mice. **F,** Morphometric analysis of pulmonary vessels in WT and NMDAR-KO mice. **Upper,** Pulmonary vessels were assigned to 4 groups on the basis of external vessel diameter (<30 μm, 30–50 μm, 50–75 μm, and 75–125 μm). Each vessel was classified as nonmuscularized, partially muscularized, or fully muscularized (n=5 mice/group). **Lower,** Representative laser scanning microscopy images of WT and NMDAR-KO mouse lung sections labeled with DAPI (nuclei in blue), for α-smooth muscle actin (green), and Von-Willebrand Factor (red) and used for quantification are shown. Scale bar: 100 μm. Arrows indicate vessels. Statistical significance was determined in a Mann-Whitney test (**A**) or in a regular 2-way ANOVA with Bonferonni correction for multiple comparisons (**B** through **F**). $^{*}P<0.05$; $^{**}P<0.01$; $^{***}P<0.001$. The values shown are medians±min to max values (**A**) or means±SEM (**B** through **F**).

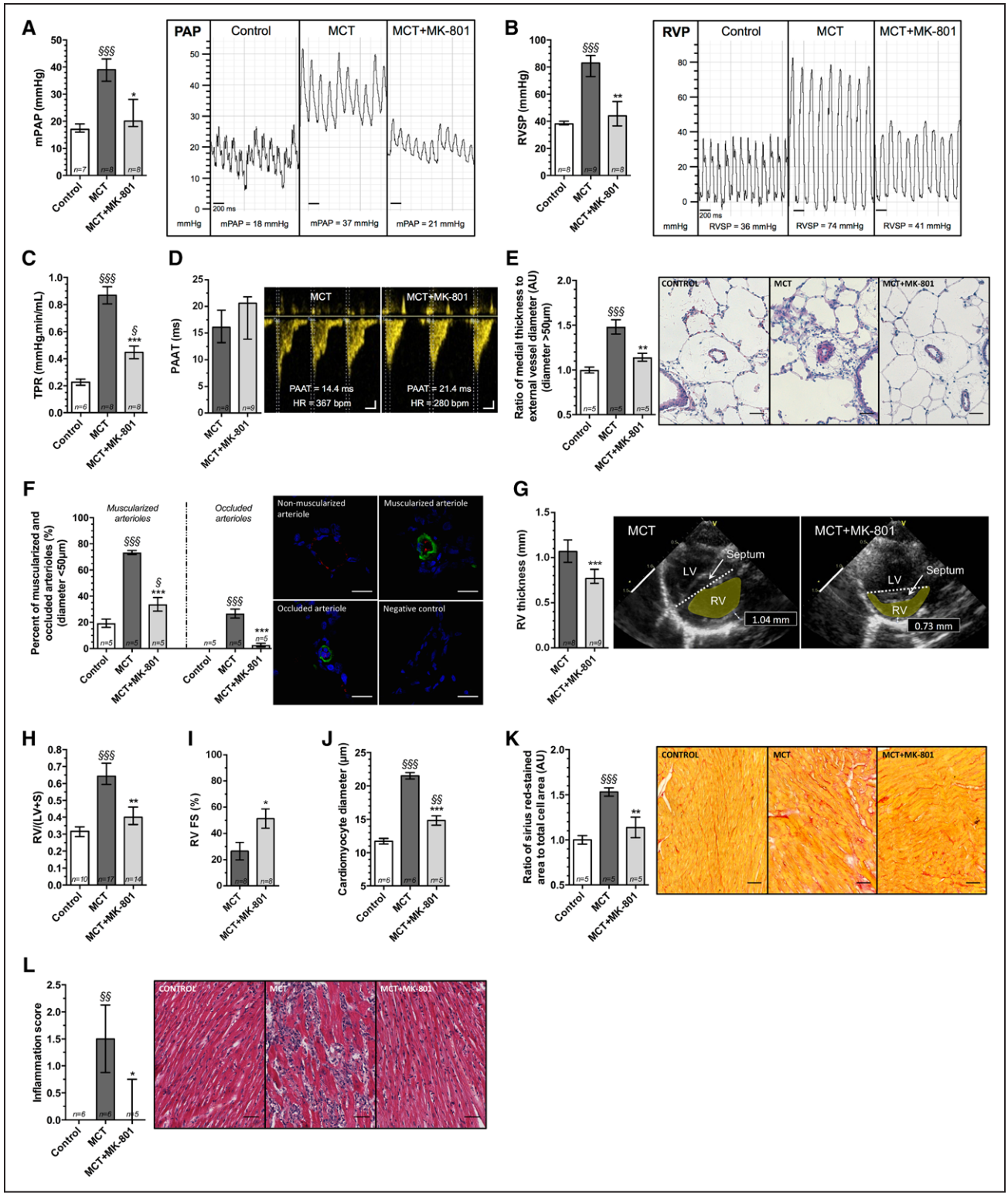

Figure 5. The NMDAR antagonist MK-801 can reverse experimental pulmonary hypertension, decreasing vascular and cardiac remodeling in the monocrotaline rat model.

Three groups of rats were compared: (1) saline-treated controls (control), (2) monocrotaline (MCT)-exposed group (MCT), and (3) MCT-exposed group treated with 3 mg·kg^{-1}·day^{-1} (days 14–21) MK-801 (MCT+MK-801). In vivo effects of MK-801 3 weeks after MCT injection. **A,** Mean pulmonary arterial pressure (mPAP, mm Hg). **Right,** Representative traces of pressure variations in the PA of control, MCT, and MCT+MK-801 rats. Scale bar: 200 ms. **B,** Right ventricular systolic pressure (RVSP, mm Hg). **Right,** Representative traces of pressure variations in the right ventricle of control, MCT, and MCT+MK-801 rats. Scale bar: 200 ms. **C,** Calculated total pulmonary vascular resistance (TPR, mm Hg·min·ml^{-1}). **D,** Pulmonary artery acceleration (*Continued*)

We also found that the ET-1/ET_AR pathway stimulated the glutamate-NMDAR axis in PASMCs. However, the endothelin receptor antagonists used in clinical practice cannot cure human PAH, despite their efficacy for improving exercise capacity, hemodynamics, and clinical outcome.[47] Almost all the patients with PAH studied here were taking endothelin receptor antagonists, but they nevertheless displayed glutamine and glutamate accumulation and high levels of GluN1 expression/phosphorylation in their hPAs. Thus, the glutamate-NMDAR axis dysregulation was apparently not influenced by ERA administration in patients with PAH probably because of the contribution of other PAH-related pathways (eg, involving PDGFR and K_v channels).

NMDAR antagonists, such as memantine and MK-801, were able to prevent or reverse experimental PH in rats. They decreased endothelial dysfunction and macrophage infiltration, consistent with observations at the CNS level, showing brain endothelial barrier permeabilization[17] and monocyte transmigration[16] after endothelial NMDAR activation. They also decreased vascular remodeling and inhibited hPASMC proliferation in vitro and proliferative cell nuclear antigen protein production in vivo in rPAs, suggesting a therapeutic effect mediated by the inhibition of SMC proliferation. MK-801 also decreased GLS1 overexpression in PAs from MCT rats, suggesting additional effects on glutamate production. These findings are consistent with those of a previous study demonstrating that GLS1 inhibition improves the course of the disease by inhibiting pulmonary vascular cell proliferation and vascular remodeling in the MCT rat model.[8] Moreover, MK-801 may act on the apoptosis-resistant phenotype of pulmonary vascular cells as they prevent the accumulation of abnormally high levels of survivin protein in MCT rPAs. Survivin is of particular importance in PASMCs because its inhibition induces PASMC apoptosis, reversing PH in the MCT rat model.[48] Because PDGFR activation triggers an increase in survivin expression in SMCs,[49] the pathological survivin overexpression found in MCT rPAs might be secondary to NMDAR overactivation in the context of NMDAR-PDGFR crosstalk. NMDAR antagonists also decreased right cardiac hypertrophy, possibly secondary to the inhibition of pulmonary vascular remodeling. However, because cardiac cells may express NMDAR,[50] NMDAR antagonists may directly modulate heart remodeling, particularly because cardiac NMDAR blockade or cardiomyocyte NMDAR deficiency have been shown to have potential protective effects on the heart.[50,51] Thus, NMDAR antagonists may correct the disease through effects on the 3 systems involved in PAH (immune, pulmonary vascular, and cardiac systems) by acting on immune inflammatory cell infiltration, vascular remodeling, and cardiac remodeling. The NMDAR antagonists we used in vivo may also have effects on vascular tone because of modulation of the autonomic nervous system,[52] contributing to the overall effect. However, the systemic pressure in treated rats was not significantly modified. Moreover, smooth muscle NMDAR-KO in mice demonstrated the actual contribution of PASMC NMDARs per se to the hypoxic vascular remodeling process. Nevertheless, NMDAR antagonists decreased EC dysfunction (assessed by determining serum-soluble E-selectin con-

Figure 5 Continued. time (PAAT) measurement by echocardiography in pulsed-wave Doppler mode in MCT and MCT+MK-801 rats. **Right,** Representative traces of blood velocity variations in the PA of MCT and MCT+MK-801 rats. Horizontal scale bar: 100 ms. Vertical scale bar: 10 cm/s. **E, Left,** Medial hypertrophy of PAs (external diameter >50 μm). **E, Right,** Representative transmitted light microscopy images of H&E-stained lung sections from control, MCT, and MCT+MK-801 rats. Scale bar: 50 μm. **F,** Morphometric analysis of small pulmonary vessels (external diameter <50 μm). Pulmonary vessels were classified into 3 groups: nonmuscularized, muscularized, and occluded arterioles. **Left,** Percentage of muscularized and occluded arterioles. **Right,** Representative laser scanning microscopy images of rat lung sections labeled with DAPI (nuclei in blue), α-smooth muscle actin (green), and Von-Willebrand Factor (red) used for quantification, providing examples of nonmuscularized, muscularized, and occluded vessels. Scale bar: 20 μm. **G,** Right ventricle thickness measured by echocardiography. **Right,** Representative parasternal short-axis views of hearts from MCT and MCT+MK-801 rats. Arrows indicate septa. Note the septal deviation toward the left ventricle in the MCT rats. Right ventricle areas are highlighted in yellow. Scale bar: 5 mm. **H,** Fulton's index of right ventricular hypertrophy, calculated as the ratio of right ventricle-to-left ventricle plus septum weight (RV/LV+S). **I,** Right ventricle fractional shortening based on echocardiographic measurement in time-motion (TM) mode for MCT and MCT+MK-801 rats. **J,** Analysis of cardiomyocyte hypertrophy as assessed by measuring cardiomyocyte diameter (μm, vertical bar) in the right heart. **K,** Analysis of cardiac fibrosis in the right heart, as assessed by the ratio of the Sirius red-stained area to the total cell area. **Left,** Graph. **Right,** Representative transmitted light microscopy images of Sirius red staining for lung sections from control, MCT, and MCT+MK-801 rats used as an example for quantification. Scale bar: 50 μm. **L,** Analysis of inflammation in the right heart. **Left,** Inflammation score as evaluated blindly by the pathologist. **Right,** Representative transmitted light microscopy images of H&E/safranin staining of lung sections from control, MCT, and MCT+MK-801 rats provided as an example of scoring. Scale bar: 50 μm. Statistical significance was determined in Mann-Whitney or Kruskal-Wallis tests followed by Dunn's multiple comparison tests (**A, B, D, G, H,** and **L**) or 1-way ANOVA followed by Bonferroni correction for multiple comparisons (**C, E, F,** and **I**–**K**). $^{§}P<0.05$; $^{§§}P<0.01$; $^{§§§}P<0.001$ versus control. $^{*}P<0.05$; $^{**}P<0.01$; $^{***}P<0.001$ versus MCT. Values are medians±interquartile range (**A, B, D, G, H,** and **L**) or means±SEM (**C, E, F,** and **I** through **K**). H&E indicates hematoxylin and eosin; HR, heart rate; NMDAR, *N*-methyl-D-aspartate receptor; PA, pulmonary artery; PAP, pulmonary arterial pressure; and RVP, right ventricular pressure.

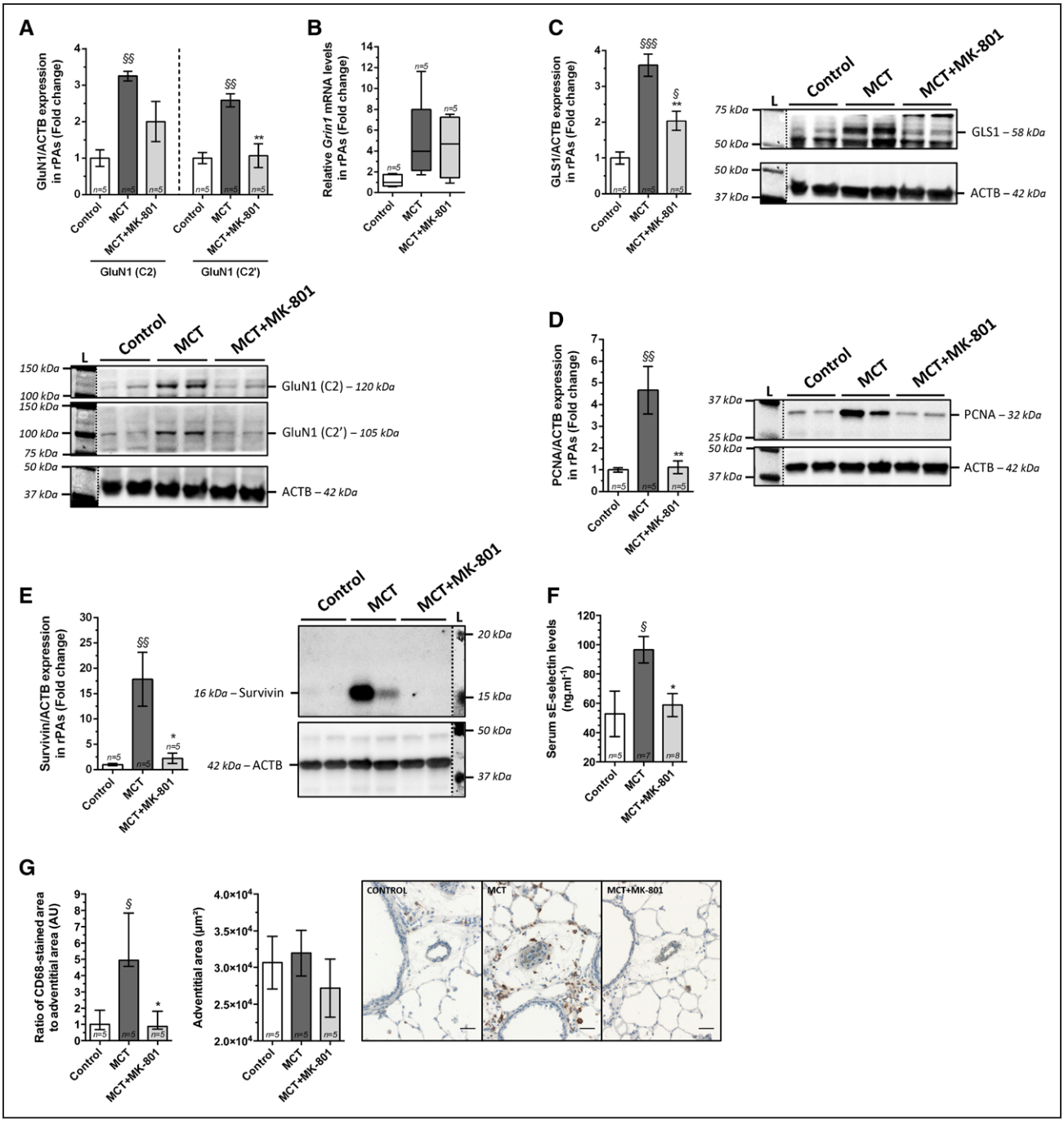

Figure 6. Effects of MK-801 on the glutamate-NMDAR axis, proliferation, apoptosis resistance, endothelial dysfunction, and inflammation in the pulmonary arteries of monocrotaline-treated rats.

The rats were from the same experiments as in Figure 5. **A, Right,** Western blot of GluN1 protein (C2 and C2′ isoforms) on lysates of isolated rPAs from control, MCT, and MCT+MK-801 rats, with normalization relative to ACTB. L indicates protein ladder. **A, Left,** Western blot quantification. Values are expressed as fold change of the mean value relative to controls. **B,** Quantitative RT-PCR of *Grin1* on total RNA from isolated PAs from control, MCT, and MCT+MK-801 rats normalized with respect to *Actb* gene expression. Values are normalized with respect to those of control rats. **C** through **E, Right,** Western blot of GLS1 (**C**), proliferative cell nuclear antigen (PCNA) (**D**), and survivin (**E**) proteins on lysates of isolated rPAs from control, MCT, and MCT+MK-801 rats with normalization relative to ACTB. L indicates protein ladder. **C** through **E, Left,** Western blot quantification. Values are expressed as fold change of the mean value relative to controls. **F,** EC dysfunction as assessed by titration of serum soluble E-selectin from control, MCT, and MCT+MK-801 rats. **G,** Analysis of adventitial inflammatory cells as assessed by CD68 immunohistochemical labeling of lung tissue macrophages in control, MCT, and MCT+MK-801 rats. **Left,** Quantification of the ratio of CD68-stained areas to adventitial areas. **Middle,** Adventitial areas. **Right,** Representative transmitted light microscopy images of CD68 staining (brown) on lung sections from control, MCT, and MCT+MK-801 rats (*Continued*)

centration) in treated rats, indicating an overall effect on vascular homeostasis. Further studies are required to determine the role of endothelial NMDARs in the vascular remodeling associated with PAH.

NMDAR blockers (eg, MK-801 and memantine) are widely used as research tools to decipher the roles of NMDARs in different organs. However, like every pharmacologically active molecule, they may have some degrees of yet unknown off-target effects in the vascular system. These drugs selectively block the NMDARs in the glutamate receptor family, but they might also act, although less potently, on other non-glutamate receptors.[50,53] We cannot completely rule out the possibility of off-target effects in our experiments, but both antagonists showed inhibitory effects on hPASMC proliferation from doses as low as 10μM (Figure 3D) and with dose-dependent effect. Also, these molecules belong to 2 different classes, therefore limiting the risk of shared off-targets. We confirmed the direct role of SMC NMDARs in pulmonary arterial remodeling and PH in SMC-targeted NMDAR KO mice, suggesting that at least part of the effects observed with NMDAR antagonists may be imputed to the NMDAR blockade.

We found that the MCT rat model was suitable for in vivo assessments of the mechanisms underlying NMDAR blockade using NMDAR antagonists mainly because it is a relevant model to explore lesions involving PASMCs, such as medial hyperplasia-type lesions. It also showed features of dysregulation of pulmonary metabolic dysregulation, including glutamate/glutamine,[54] and the glutamate/NMDAR pathways, similar to that in human PAH. However, the MCT model does not recapitulate the full spectrum of typical PAH lesions, such as the so-called plexogenic ones, and may not well predict the future response to therapy in human PAH. Thus, in a translational perspective, other animal models triggering more severe experimental PH, such as MCT+pneumonectomy model, or allowing more prolonged treatment, such as the Sugen/hypoxia, both displaying more complex lesion types than the MCT model, could be used.[55]

Several milestones must be attained before these findings can be transferred into clinical practice. MK-801 and memantine had beneficial effects on experimental PH, but they may have adverse central effects, rendering them unsuitable for PAH treatment in humans. Dextromethorphan, an over-the-counter drug with NMDAR antagonist activity, has recently been evaluated in type 2 diabetes mellitus in a phase IIa clinical trial.[56] Only moderate adverse effects were observed in the short term, but chronic intake would require close monitoring because, at high doses, this drug can impair working memory, disrupt locomotion, and induce moderate ataxia.[57] Ketamine, a known NMDAR antagonist with pulmonary vasodilatory potential, was not associated with changes in pulmonary hemodynamics in children with PH when used as an anesthetic.[58,59] Its central catecholamine-mediated effect may explain the absence of a net effect on pulmonary arterial pressure. Moreover, ketamine has a complex pharmacology, with effects on multiple CNS targets, potentially limiting its long-term use to combat vascular remodeling.

It would, therefore, not be appropriate to test these molecules for long-term administration. Specific therapeutic tools, such as NMDAR antagonists targeting the peripheral receptor with minimal central effects, would be useful in PAH and other disorders involving NMDAR activation outside the CNS, such as some cancers[21–23] and diabetes mellitus.[13,56] Such NMDAR antagonists that do not cross the blood-brain barrier are currently under development in a lead optimization phase (see notes on patents).

Peripheral NMDARs may also contribute to different physiological functions, for instance, promoting pain transmission, amplifying platelet activation and aggregation, increasing glucose-stimulated insulin release, regulating bone desorption and resorption, and so on (for reviews, see Hogan-Cann & Anderson[60] and Zhou et al[61]). Although recent articles indicate that NMDAR blockade does not induce spontaneous bleeding or hypoglycemia, the critical effects of NMDAR blockade on these physiological functions need to be clarified.[13,62] To limit the potential peripheral side effects of nonselective NMDAR blockade, if any, a strategy aiming to identify the NMDAR subtype(s) that promote(s) vascular remodeling in PAH, mirroring the current approach for CNS disorders, could be used.

Overall, the glutamate accumulation in PAH hPAs, the increased glutamate release from hPASMCs secondary to ETAR activation and K_v channel shutdown, and the increased expression and phosphorylation of NMDAR in PAH hPAs are consistent with engagement and overactivation of the glutamate/NMDAR axis in PAH hPAs. No antiremodeling strategy has yet been approved for PAH, but the use of appropriate NMDAR antagonists may improve PAH by antiremodeling effects.

Figure 6 Continued. counterstained with hematoxylin (blue) and used as an example for quantification. Scale bar: 50 μm. Statistical significance was determined in Kruskal-Wallis tests followed by Dunn's multiple comparison tests (**B** and **G**) or 1-way ANOVA with Bonferroni correction for multiple comparisons (**A** and **C** through **F**). $^{§}P<0.05$; $^{§§}P<0.01$; $^{§§§}P<0.001$ versus control. $^{*}P<0.05$; $^{**}P<0.01$ versus MCT. Values are means±SEM (**A** and **C** through **F**), medians±min to max values (**B**), or medians ± interquartile range (**G**). ACTB indicates beta actin; GLS1, glutaminase 1; NMDAR, *N*-methyl-D-aspartate receptor; PA, pulmonary artery; and rPA, rat pulmonary artery.

Peripheral NMDARs are, therefore, potential targets for therapeutic intervention in PAH.

ARTICLE INFORMATION

Received June 13, 2017; accepted December 22, 2017.

The online-only Data Supplement, podcast, and transcript are available with this article at http://circ.ahajournals.org/lookup/suppl/doi:10.1161/CIRCULATIONAHA.117.029930/-/DC1.

Correspondence

Sylvia Cohen-Kaminsky, PhD, Hôpital Marie Lannelongue, INSERM UMR-S 999, 133 Avenue de la résistance, 92350 Le Plessis-Robinson, France. E-mail sylvia.cohen-kaminsky@u-psud.fr

Affiliations

INSERM UMR-S 999, Hôpital Marie Lannelongue, Le Plessis-Robinson, France (S.J.D., G.B.-M., A.C., M.Q., C.R.-M, F.A., M.K.N., B.R., E.G., M.-C.V., M.V., N.R., P.D., E.F., F.P., M.H., S.C.-K.). University Paris-Sud, Faculté de Médecine, Université Paris-Saclay, Le Kremlin-Bicêtre, France (S.J.D., G.B.-M., A.C., M.Q., C.R.-M, F.A., M.K.N., B.R., E.G., M.-C.V., M.V., N.R., P.D., E.F., F.P., M.H., S.C.-K.). AP-HP Assistance Publique-Hôpitaux de Paris, Service de Pneumologie, Hôpital Bicêtre, Le Kremlin-Bicêtre, France (M.H.).

Acknowledgments

The authors thank J. Burlot, P. Robert, and V. Domergue (animal core facility ANIMEX, Institut Paris Saclay d'Innovation Thérapeutique, Université Paris-Sud), B. Decante (animal core facility of Hôpital Marie Lannelongue), A. Solgadi, S. Nicolaÿ, and P. Chaminade (Institut Paris Saclay d'Innovation Thérapeutique mass spectrometry facility SAMM), G. Hamm, F. Pamelard, and J. Stauber from ImaBiotech (www.imabiotech.com) for MSI experiments, and B. Besson-Lescure and N. Meunier-Brunel from INSERM IFR 65 (Plateforme de Microdosages, Paris, France) for Milliplex analysis. The authors also thank Prof O. Mercier, Dr S. Mussot, and Dr D. Fabre, surgeons in the Service de chirurgie thoracique & vasculaire from Hôpital Marie Lannelongue, for providing human lung tissues, and F. Lecerf and J. Arthur for preparing primary lung vascular cells. The authors thank the French Pulmonary Hypertension Registry facilities and the French National Referral Center for Severe Pulmonary Hypertension for providing clinical samples and data. The authors thank V. Capuano and C. Communaux for technical assistance, J. F. Renaud de la Faverie for continuous support, Y. Dutheil for administrative assistance, and I. Klingel-Schmitt for technical assistance, before her untimely death. The authors thank J. Sappa (Alex Edelman & Associates) for professional biomedical English editing. S.C.-K. supervised and coordinated the study, and S.J.D. and S.C.-K. designed the experiments and wrote the article. S.J.D., G.B.-M., M.Q., E.G., and C.R.-M. set up in vitro experiments, S.J.D, G.B.-M, M.Q., M.-C.V., M.V., N.R., and A.C. performed in vitro experiments, and S.J.D. and G.B.-M. analyzed the results. S.J.D., F.P., G.B.-M., and A.C. set up in vivo experiments, S.J.D., F.P., A.C., and B.R. performed in vivo experiments, and S.J.D., F.P., C.R.-M., and P.D. analyzed the results. S.J.D. performed the MSI experiments in collaboration with ImaBiotech and liquid chromatography-tandem mass spectrometry experiments on the SAMM platform. F.A. and F.P. provided distal hPAs, hPMVECs, and hPASMCs from patients with PAH and controls. M.H., head of the National Reference Center for PAH, made available patient samples and clinical data and participated in helpful discussions. Lung tissues were made available from our tissue bank under the responsibility of E.F. and P.D. Also, S.J.D. received specific training on statistics and did most of the statistical analysis, with the support of M.K.N. All authors approved the article.

Sources of Funding

The NUTS project (NMDA Receptors, Unexpected Targets in Pulmonary Arterial Hypertension) is supported by LabEx LERMIT, Laboratory of Excellence in Research on Medication and Innovative Therapeutics under the Investment for the Future program Agence Nationale de la Recherche (ANR)-11-IDEX-0003-01 within the ANR-10-LABX-0033 (to S.C.-K.), the Excellence Initiative IDEX Paris-Saclay Prématuration program (to S.C.-K.), ANR Biomedical Innovation program 2014 (DS0404) within ANR-14-CE16-0016 (to S.C.-K.), Département Hospitalo-Universitaire Thorax Innovation, and Assistance Publique-Hôpitaux de Paris. This work was also funded by Institut National de la Santé Et de la Recherche Médicale (INSERM), Université Paris-Sud, and Hôpital Marie Lannelongue. We thank Région Ile-de-France and Université Paris-Sud for providing financial support for Institut Paris Saclay d'Innovation Thérapeutique (IPSIT) facilities. The sponsors had no role in the design of the study, the collection and analysis of the data, or the preparation of the article. S.J.D. received doctoral support from Fonds de Dotation Recherche en Santé Respiratoire and Fondation pour la Recherche Médicale (grant FDT20140931207). F.P. was supported by the ANR (grant ANR-13-JSV1-0011), F.A. by a postdoctoral grant from Aviesan (Alliance nationale pour les sciences de la vie et de la santé, Institut Immunologie, Hématologie et Pneumologie), M.Q. by a PhD fellowship from the Ministère de l'Education Nationale, de l'Enseignement Supérieur et de la Recherche, B.R. by a doctoral grant from LabEx LERMIT, Laboratory of Excellence in Research on Medication and Innovative Therapeutics, A.C. by a postdoctoral fellowship from Fondation pour la Recherche Médicale (grant SPF20140129310), MN by a postdoctoral fellowship from INSERM, and G.B.-M. by a postdoctoral fellowship from LabEx LERMIT, Laboratory of Excellence in Research on Medication and Innovative Therapeutics.

Disclosures

S.C.-K., M.H., G.B.-M., and S.J.D. have filed International Patent Applications WO2017017116A1 (published February 2, 2017) and WO/2017/216159 (published December 21, 2017) concerning novel NMDAR antagonists targeting peripheral NMDARs. M.H. has a relationship with Actelion, Bayer, GSK, Novartis, and Pfizer. In addition to being an investigator in trials involving these companies, he provides them with consultancy services and is a member of scientific advisory boards. The other authors report no conflicts of interest.

REFERENCES

1. Galiè N, Humbert M, Vachiery JL, Gibbs S, Lang I, Torbicki A, Simonneau G, Peacock A, Vonk Noordegraaf A, Beghetti M, Ghofrani A, Gomez Sanchez MA, Hansmann G, Klepetko W, Lancellotti P, Matucci M, McDonagh T, Pierard LA, Trindade PT, Zompatori M, Hoeper M. 2015 ESC/ERS guidelines for the diagnosis and treatment of pulmonary hypertension: the Joint Task Force for the Diagnosis and Treatment of Pulmonary Hypertension of the European Society of Cardiology (ESC) and the European Respiratory Society (ERS): endorsed by Association for European Paediatric and Congenital Cardiology (AEPC), International Society for Heart and Lung Transplantation (ISHLT). *Eur Respir J*. 2015;46:903–975. doi: 10.1183/13993003.01032-2015.
2. Schermuly RT, Ghofrani HA, Wilkins MR, Grimminger F. Mechanisms of disease: pulmonary arterial hypertension. *Nat Rev Cardiol*. 2011;8:443–455. doi: 10.1038/nrcardio.2011.87.
3. Humbert M, Lau EM, Montani D, Jaïs X, Sitbon O, Simonneau G. Advances in therapeutic interventions for patients with pulmonary arterial hypertension. *Circulation*. 2014;130:2189–2208. doi: 10.1161/CIRCULATIONAHA.114.006974.
4. Sutendra G, Michelakis ED. Pulmonary arterial hypertension: challenges in translational research and a vision for change. *Sci Transl Med*. 2013;5:208sr5. doi: 10.1126/scitranslmed.3005428.
5. Ranchoux B, Antigny F, Rucker-Martin C, Hautefort A, Péchoux C, Bogaard HJ, Dorfmüller P, Remy S, Lecerf F, Planté S, Chat S, Fadel E, Houssaini A, Anegon I, Adnot S, Simonneau G, Humbert M, Cohen-Kaminsky S, Perros F. Endothelial-to-mesenchymal transition in pulmonary hypertension. *Circulation*. 2015;131:1006–1018. doi: 10.1161/CIRCULATIONAHA.114.008750.
6. Paulin R, Michelakis ED. The metabolic theory of pulmonary arterial hypertension. *Circ Res*. 2014;115:148–164. doi: 10.1161/CIRCRESAHA.115.301130.
7. Sutendra G, Bonnet S, Rochefort G, Haromy A, Folmes KD, Lopaschuk GD, Dyck JRB, Michelakis ED. Fatty acid oxidation and malonyl-CoA decarboxylase in the vascular remodeling of pulmonary hypertension. *Sci Transl Med*. 2010;2:44ra58. doi: 10.1126/scitranslmed.3001327.
8. Bertero T, Oldham WM, Cottrill KA, Pisano S, Vanderpool RR, Yu Q, Zhao J, Tai Y, Tang Y, Zhang YY, Rehman S, Sugahara M, Qi Z, Gorcsan J III, Vargas SO, Saggar R, Saggar R, Wallace WD, Ross DJ, Haley KJ, Waxman AB, Parikh VN, De Marco T, Hsue PY, Morris A, Simon MA, Norris KA, Gaggioli C, Loscalzo J, Fessel J, Chan SY. Vascular stiffness mechanoactivates YAP/TAZ-dependent glutaminolysis to drive pulmonary hypertension. *J Clin Invest*. 2016;126:3313–3335. doi: 10.1172/JCI86387.
9. Egnatchik RA, Brittain EL, Shah AT, Fares WH, Ford HJ, Monahan K, Kang CJ, Kocurek EG, Zhu S, Luong T, Nguyen TT, Hysinger E, Austin ED, Skala MC, Young JD, Roberts LJ, Hemnes AR, West J, Fessel JP. Dysfunctional BMPR2 signaling drives an abnormal endothelial requirement for glutamine in pulmonary arterial hypertension. *Pulm Circ*. 2017;7:186–199. doi: 10.1086/690236.

10. Nedergaard M, Takano T, Hansen AJ. Beyond the role of glutamate as a neurotransmitter. *Nat Rev Neurosci*. 2002;3:748–755. doi: 10.1038/nrn916.
11. Bozic M, Valdivielso JM. The potential of targeting NMDA receptors outside the CNS. *Expert Opin Ther Targets*. 2015;19:399–413. doi: 10.1517/14728222.2014.983900.
12. Affaticati P, Mignen O, Jambou F, Potier MC, Klingel-Schmitt I, Degrouard J, Peineau S, Gouadon E, Collingridge GL, Liblau R, Capiod T, Cohen-Kaminsky S. Sustained calcium signalling and caspase-3 activation involve NMDA receptors in thymocytes in contact with dendritic cells. *Cell Death Differ*. 2011;18:99–108. doi: 10.1038/cdd.2010.79.
13. Marquard J, Otter S, Welters A, Stirban A, Fischer A, Eglinger J, Herebian D, Kletke O, Klemen MS, Stožer A, Wnendt S, Piemonti L, Köhler M, Ferrer J, Thorens B, Schliess F, Rupnik MS, Heise T, Berggren PO, Klöcker N, Meissner T, Mayatepek E, Eberhard D, Kragl M, Lammert E. Characterization of pancreatic NMDA receptors as possible drug targets for diabetes treatment. *Nat Med*. 2015;21:363–372. doi: 10.1038/nm.3822.
14. Sharp CD, Houghton J, Elrod JW, Warren A, Jackson TH IV, Jawahar A, Nanda A, Minagar A, Alexander JS. N-methyl-D-aspartate receptor activation in human cerebral endothelium promotes intracellular oxidant stress. *Am J Physiol Heart Circ Physiol*. 2005;288:H1893–H1899. doi: 10.1152/ajpheart.01110.2003.
15. Chen H, Fitzgerald R, Brown AT, Qureshi I, Breckenridge J, Kazi R, Wang Y, Wu Y, Zhang X, Mukunyadzi P, Eidt J, Moursi MM. Identification of a homocysteine receptor in the peripheral endothelium and its role in proliferation. *J Vasc Surg*. 2005;41:853–860. doi: 10.1016/j.jvs.2005.02.021.
16. Reijerkerk A, Kooij G, van der Pol SM, Leyen T, Lakeman K, van Het Hof B, Vivien D, de Vries HE. The NR1 subunit of NMDA receptor regulates monocyte transmigration through the brain endothelial cell barrier. *J Neurochem*. 2010;113:447–453. doi: 10.1111/j.1471-4159.2010.06598.x.
17. András IE, Deli MA, Veszelka S, Hayashi K, Hennig B, Toborek M. The NMDA and AMPA/KA receptors are involved in glutamate-induced alterations of occludin expression and phosphorylation in brain endothelial cells. *J Cereb Blood Flow Metab*. 2007;27:1431–1443. doi: 10.1038/sj.jcbfm.9600445.
18. Qureshi I, Chen H, Brown AT, Fitzgerald R, Zhang X, Breckenridge J, Kazi R, Crocker AJ, Stühlinger MC, Lin K, Cooke JP, Eidt JF, Moursi MM. Homocysteine-induced vascular dysregulation is mediated by the NMDA receptor. *Vasc Med*. 2005;10:215–223. doi: 10.1191/1358863x05vm626oa.
19. Doronzo G, Russo I, Del Mese P, Viretto M, Mattiello L, Trovati M, Anfossi G. Role of NMDA receptor in homocysteine-induced activation of mitogen-activated protein kinase and phosphatidyl inositol 3-kinase pathways in cultured human vascular smooth muscle cells. *Thromb Res*. 2010;125:e23–e32. doi: 10.1016/j.thromres.2009.08.015.
20. Paoletti P, Bellone C, Zhou Q. NMDA receptor subunit diversity: impact on receptor properties, synaptic plasticity and disease. *Nat Rev Neurosci*. 2013;14:383–400. doi: 10.1038/nrn3504.
21. Li L, Hanahan D. Hijacking the neuronal NMDAR signaling circuit to promote tumor growth and invasion. *Cell*. 2013;153:86–100. doi: 10.1016/j.cell.2013.02.051.
22. Stepulak A, Sifringer M, Rzeski W, Endesfelder S, Gratopp A, Pohl EE, Bittigau P, Felderhoff-Mueser U, Kaindl AM, Bührer C, Hansen HH, Stryjecka-Zimmer M, Turski L, Ikonomidou C. NMDA antagonist inhibits the extracellular signal-regulated kinase pathway and suppresses cancer growth. *Proc Natl Acad Sci U S A*. 2005;102:15605–15610. doi: 10.1073/pnas.0507679102.
23. Takano T, Lin JH, Arcuino G, Gao Q, Yang J, Nedergaard M. Glutamate release promotes growth of malignant gliomas. *Nat Med*. 2001;7:1010–1015. doi: 10.1038/nm0901-1010.
24. Guignabert C, Tu L, Le Hiress M, Ricard N, Sattler C, Seferian A, Huertas A, Humbert M, Montani D. Pathogenesis of pulmonary arterial hypertension: lessons from cancer. *Eur Respir Rev*. 2013;22:543–551. doi: 10.1183/09059180.00007513.
25. Scott DB, Blanpied TA, Swanson GT, Zhang C, Ehlers MD. An NMDA receptor ER retention signal regulated by phosphorylation and alternative splicing. *J Neurosci*. 2001;21:3063–3072.
26. Lau CG, Zukin RS. NMDA receptor trafficking in synaptic plasticity and neuropsychiatric disorders. *Nat Rev Neurosci*. 2007;8:413–426. doi: 10.1038/nrn2153.
27. Xu H, Bae M, Tovar-y-Romo LB, Patel N, Bandaru VV, Pomerantz D, Steiner JP, Haughey NJ. The human immunodeficiency virus coat protein gp120 promotes forward trafficking and surface clustering of NMDA receptors in membrane microdomains. *J Neurosci*. 2011;31:17074–17090. doi: 10.1523/JNEUROSCI.4072-11.2011.
28. Takamori S, Rhee JS, Rosenmund C, Jahn R. Identification of a vesicular glutamate transporter that defines a glutamatergic phenotype in neurons. *Nature*. 2000;407:189–194. doi: 10.1038/35025070.
29. Archer SL, Weir EK, Wilkins MR. Basic science of pulmonary arterial hypertension for clinicians: new concepts and experimental therapies. *Circulation*. 2010;121:2045–2066. doi: 10.1161/CIRCULATIONAHA.108.847707.
30. Giaid A, Yanagisawa M, Langleben D, Michel RP, Levy R, Shennib H, Kimura S, Masaki T, Duguid WP, Stewart DJ. Expression of endothelin-1 in the lungs of patients with pulmonary hypertension. *N Engl J Med*. 1993;328:1732–1739. doi: 10.1056/NEJM199306173282402.
31. Sasaki Y, Takimoto M, Oda K, Früh T, Takai M, Okada T, Hori S. Endothelin evokes efflux of glutamate in cultures of rat astrocytes. *J Neurochem*. 1997;68:2194–2200.
32. Moudgil R, Michelakis ED, Archer SL. The role of k+ channels in determining pulmonary vascular tone, oxygen sensing, cell proliferation, and apoptosis: implications in hypoxic pulmonary vasoconstriction and pulmonary arterial hypertension. *Microcirc N Y N 1994*. 2006;13:615–632.
33. Beazely MA, Lim A, Li H, Trepanier C, Chen X, Sidhu B, Macdonald JF. Platelet-derived growth factor selectively inhibits NR2B-containing N-methyl-D-aspartate receptors in CA1 hippocampal neurons. *J Biol Chem*. 2009;284:8054–8063. doi: 10.1074/jbc.M805384200.
34. Perros F, Montani D, Dorfmüller P, Durand-Gasselin I, Tcherakian C, Le Pavec J, Mazmanian M, Fadel E, Mussot S, Mercier O, Hervé P, Emilie D, Eddahibi S, Simonneau G, Souza R, Humbert M. Platelet-derived growth factor expression and function in idiopathic pulmonary arterial hypertension. *Am J Respir Crit Care Med*. 2008;178:81–88. doi: 10.1164/rccm.200707-1037OC.
35. Andiné P, Widermark N, Axelsson R, Nyberg G, Olofsson U, Mårtensson E, Sandberg M. Characterization of MK-801-induced behavior as a putative rat model of psychosis. *J Pharmacol Exp Ther*. 1999;290:1393–1408.
36. Moyanova SG, Kortenska LV, Mitreva RG, Pashova VD, Ngomba RT, Nicoletti F. Multimodal assessment of neuroprotection applied to the use of MK-801 in the endothelin-1 model of transient focal brain ischemia. *Brain Res*. 2007;1153:58–67. doi: 10.1016/j.brainres.2007.03.070.
37. Antigny F, Hautefort A, Meloche J, Belacel-Ouari M, Manoury B, Rucker-Martin C, Péchoux C, Potus F, Nadeau V, Tremblay E, Ruffenach G, Bourgeois A, Dorfmüller P, Breuils-Bonnet S, Fadel E, Ranchoux B, Jourdon P, Girerd B, Montani D, Provencher S, Bonnet S, Simonneau G, Humbert M, Perros F. Potassium Channel Subfamily K Member 3 (KCNK3) contributes to the development of pulmonary arterial hypertension. *Circulation*. 2016;133:1371–1385. doi: 10.1161/CIRCULATIONAHA.115.020951.
38. Kalev-Zylinska ML, Green TN, Morel-Kopp MC, Sun PP, Park YE, Lasham A, During MJ, Ward CM. N-methyl-D-aspartate receptors amplify activation and aggregation of human platelets. *Thromb Res*. 2014;133:837–847. doi: 10.1016/j.thromres.2014.02.011.
39. Collard CD, Park KA, Montalto MC, Alapati S, Buras JA, Stahl GL, Colgan SP. Neutrophil-derived glutamate regulates vascular endothelial barrier function. *J Biol Chem*. 2002;277:14801–14811. doi: 10.1074/jbc.M110557200.
40. Speyer CL, Hachem AH, Assi AA, Johnson JS, DeVries JA, Gorski DH. Metabotropic glutamate receptor-1 as a novel target for the antiangiogenic treatment of breast cancer. *PLoS One*. 2014;9:e88830. doi: 10.1371/journal.pone.0088830.
41. Yamada S, Nelson WJ. Synapses: sites of cell recognition, adhesion, and functional specification. *Annu Rev Biochem*. 2007;76:267–294. doi: 10.1146/annurev.biochem.75.103004.142811.
42. Bottos A, Destro E, Rissone A, Graziano S, Cordara G, Assenzio B, Cera MR, Mascia L, Bussolino F, Arese M. The synaptic proteins neurexins and neuroligins are widely expressed in the vascular system and contribute to its functions. *Proc Natl Acad Sci U S A*. 2009;106:20782–20787. doi: 10.1073/pnas.0809510106.
43. Germain M, Eyries M, Montani D, Poirier O, Girerd B, Dorfmüller P, Coulet F, Nadaud S, Maugenre S, Guignabert C, Carpentier W, Vonk-Noordegraaf A, Lévy M, Chaouat A, Lambert J-C, Bertrand M, Dupuy A-M, Letenneur L, Lathrop M, Amouyel P, de Ravel TJL, Delcroix M, Austin ED, Robbins IM, Hemnes AR, Loyd JE, Berman-Rosenzweig E, Barst RJ, Chung WK, Simonneau G, Trégouët DA, Humbert M, Soubrier F. Genome-wide association analysis identifies a susceptibility locus for pulmonary arterial hypertension. *Nat Genet*. 2013;45:518–521.
44. Anaparti V, Pascoe CD, Jha A, Mahood TH, Ilarraza R, Unruh H, Moqbel R, Halayko AJ. Tumor necrosis factor regulates NMDA receptor-mediated airway smooth muscle contractile function and airway responsiveness. *Am J Physiol Lung Cell Mol Physiol*. 2016;311:L467–L480. doi: 10.1152/ajplung.00382.2015.

45. Betzen C, White R, Zehendner CM, Pietrowski E, Bender B, Luhmann HJ, Kuhlmann CR. Oxidative stress upregulates the NMDA receptor on cerebrovascular endothelium. *Free Radic Biol Med*. 2009;47:1212–1220. doi: 10.1016/j.freeradbiomed.2009.07.034.
46. Zhang J, Zhong W, Cui T, Yang M, Hu X, Xu K, Xie C, Xue C, Gibbons GH, Liu C, Li L, Chen YE. Generation of an adult smooth muscle cell-targeted Cre recombinase mouse model. *Arterioscler Thromb Vasc Biol*. 2006;26:e23–e24. doi: 10.1161/01.ATV.0000202661.61837.93.
47. Chaumais MC, Guignabert C, Savale L, Jaïs X, Boucly A, Montani D, Simonneau G, Humbert M, Sitbon O. Clinical pharmacology of endothelin receptor antagonists used in the treatment of pulmonary arterial hypertension. *Am J Cardiovasc Drugs*. 2015;15:13–26. doi: 10.1007/s40256-014-0095-y.
48. McMurtry MS, Archer SL, Altieri DC, Bonnet S, Haromy A, Harry G, Bonnet S, Puttagunta L, Michelakis ED. Gene therapy targeting survivin selectively induces pulmonary vascular apoptosis and reverses pulmonary arterial hypertension. *J Clin Invest*. 2005;115:1479–1491.
49. Blanc-Brude OP, Yu J, Simosa H, Conte MS, Sessa WC, Altieri DC. Inhibitor of apoptosis protein survivin regulates vascular injury. *Nat Med*. 2002;8:987–994. doi: 10.1038/nm750.
50. Makhro A, Tian Q, Kaestner L, Kosenkov D, Faggian G, Gassmann M, Schwarzwald C, Bogdanova A. Cardiac N-methyl D-aspartate receptors as a pharmacological target. *J Cardiovasc Pharmacol*. 2016;68:356–373. doi: 10.1097/FJC.0000000000000424.
51. Moshal KS, Kumar M, Tyagi N, Mishra PK, Metreveli N, Rodriguez WE, Tyagi SC. Restoration of contractility in hyperhomocysteinemia by cardiac-specific deletion of NMDA-R1. *Am J Physiol Heart Circ Physiol*. 2009;296:H887–H892. doi: 10.1152/ajpheart.00750.2008.
52. Ye ZY, Li DP, Li L, Pan HL. Protein kinase CK2 increases glutamatergic input in the hypothalamus and sympathetic vasomotor tone in hypertension. *J Neurosci*. 2011;31:8271–8279. doi: 10.1523/JNEUROSCI.1147-11.2011.
53. Traynelis SF, Wollmuth LP, McBain CJ, Menniti FS, Vance KM, Ogden KK, Hansen KB, Yuan H, Myers SJ, Dingledine R. Glutamate receptor ion channels: structure, regulation, and function. *Pharmacol Rev*. 2010;62:405–496. doi: 10.1124/pr.109.002451.
54. Rafikova O, Meadows ML, Kinchen JM, Mohney RP, Maltepe E, Desai AA, Yuan JX, Garcia JG, Fineman JR, Rafikov R, Black SM. Metabolic changes precede the development of pulmonary hypertension in the monocrotaline exposed rat lung. *PLoS One*. 2016;11:e0150480. doi: 10.1371/journal.pone.0150480.
55. Maarman G, Lecour S, Butrous G, Thienemann F, Sliwa K. A comprehensive review: the evolution of animal models in pulmonary hypertension research; are we there yet? *Pulm Circ*. 2013;3:739–756. doi: 10.1086/674770.
56. Marquard J, Stirban A, Schliess F, Sievers F, Welters A, Otter S, Fischer A, Wnendt S, Meissner T, Heise T, Lammert E. Effects of dextromethorphan as add-on to sitagliptin on blood glucose and serum insulin concentrations in individuals with type 2 diabetes mellitus: a randomized, placebo-controlled, double-blinded, multiple crossover, single-dose clinical trial. *Diabetes Obes Metab*. 2016;18:100–103. doi: 10.1111/dom.12576.
57. Dematteis M, Lallement G, Mallaret M. Dextromethorphan and dextrorphan in rats: common antitussives: different behavioural profiles. *Fundam Clin Pharmacol*. 1998;12:526–537.
58. Friesen RH, Twite MD, Nichols CS, Cardwell KA, Pan Z, Darst JR, Wilson N, Fagan TE, Miyamoto SD, Ivy DD. Hemodynamic response to ketamine in children with pulmonary hypertension. *Paediatr Anaesth*. 2016;26:102–108. doi: 10.1111/pan.12799.
59. Maruyama K, Maruyama J, Yokochi A, Muneyuki M, Miyasaka K. Vasodilatory effects of ketamine on pulmonary arteries in rats with chronic hypoxic pulmonary hypertension. *Anesth Analg*. 1995;80:786–792.
60. Hogan-Cann AD, Anderson CM. Physiological roles of non-neuronal NMDA receptors. *Trends Pharmacol Sci*. 2016;37:750–767. doi: 10.1016/j.tips.2016.05.012.
61. Zhou HY, Chen SR, Pan HL. Targeting N-methyl-D-aspartate receptors for treatment of neuropathic pain. *Expert Rev Clin Pharmacol*. 2011;4:379–388.
62. Green TN, Hamilton JR, Morel-Kopp MC, Zheng Z, Chen TT, Hearn JI, Sun PP, Flanagan JU, Young D, Barber PA, During MJ, Ward CM, Kalev-Zylinska ML. Inhibition of NMDA receptor function with an anti-GluN1-S2 antibody impairs human platelet function and thrombosis. *Platelets*. 2017;28:799–811. doi: 10.1080/09537104.2017.1280149.